PD IEC/TR 61282-9:2016

BSI Standards Publication

Fibre optic communication system design guides

Part 9: Guidance on polarization mode dispersion measurements and theory

bsi.

...making excellence a habit.™

National foreword

This Published Document is the UK implementation of IEC/TR 61282-9:2016. It supersedes PD IEC/TR 61282-9:2006 which is withdrawn.

The UK participation in its preparation was entrusted by Technical Committee GEL/86, Fibre optics, to Subcommittee GEL/86/3, Fibre optic systems and active devices.

A list of organizations represented on this committee can be obtained on request to its secretary.

This publication does not purport to include all the necessary provisions of a contract. Users are responsible for its correct application.

Published by BSI Standards Limited 2016

ISBN 978 0 580 89393 3
ICS 33.180.01

Compliance with a British Standard cannot confer immunity from legal obligations.

This Published Document was published under the authority of the Standards Policy and Strategy Committee on 30 April 2016.

Amendments/corrigenda issued since publication

Date	Text affected

IEC TR 61282-9

Edition 2.0 2016-03

TECHNICAL REPORT

colour inside

Fibre optic communication system design guides – Part 9: Guidance on polarization mode dispersion measurements and theory

INTERNATIONAL ELECTROTECHNICAL COMMISSION

ICS 33.180.01

ISBN 978-2-8322-3236-1

CONTENTS

INTERNATIONAL ELECTROTECHNICAL COMMISSION

_____

FIBRE OPTIC COMMUNICATION SYSTEM DESIGN GUIDES –

Part 9: Guidance on polarization mode dispersion measurements and theory

FOREWORD

1) The International Electrotechnical Commission (IEC) is a worldwide organization for standardization comprising all national electrotechnical committees (IEC National Committees). The object of IEC is to promote international co-operation on all questions concerning standardization in the electrical and electronic fields. To this end and in addition to other activities, IEC publishes International Standards, Technical Specifications, Technical Reports, Publicly Available Specifications (PAS) and Guides (hereafter referred to as “IEC Publication(s)”). Their preparation is entrusted to technical committees; any IEC National Committee interested in the subject dealt with may participate in this preparatory work. International, governmental and non-governmental organizations liaising with the IEC also participate in this preparation. IEC collaborates closely with the International Organization for Standardization (ISO) in accordance with conditions determined by agreement between the two organizations.
2) The formal decisions or agreements of IEC on technical matters express, as nearly as possible, an international consensus of opinion on the relevant subjects since each technical committee has representation from all interested IEC National Committees.
3) IEC Publications have the form of recommendations for international use and are accepted by IEC National Committees in that sense. While all reasonable efforts are made to ensure that the technical content of IEC Publications is accurate, IEC cannot be held responsible for the way in which they are used or for any misinterpretation by any end user.
4) In order to promote international uniformity, IEC National Committees undertake to apply IEC Publications transparently to the maximum extent possible in their national and regional publications. Any divergence between any IEC Publication and the corresponding national or regional publication shall be clearly indicated in the latter.
5) IEC itself does not provide any attestation of conformity. Independent certification bodies provide conformity assessment services and, in some areas, access to IEC marks of conformity. IEC is not responsible for any services carried out by independent certification bodies.
6) All users should ensure that they have the latest edition of this publication.
7) No liability shall attach to IEC or its directors, employees, servants or agents including individual experts and members of its technical committees and IEC National Committees for any personal injury, property damage or other damage of any nature whatsoever, whether direct or indirect, or for costs (including legal fees) and expenses arising out of the publication, use of, or reliance upon, this IEC Publication or any other IEC Publications.
8) Attention is drawn to the Normative references cited in this publication. Use of the referenced publications is indispensable for the correct application of this publication.
9) Attention is drawn to the possibility that some of the elements of this IEC Publication may be the subject of patent rights. IEC shall not be held responsible for identifying any or all such patent rights.

The main task of IEC technical committees is to prepare International Standards. However, a technical committee may propose the publication of a technical report when it has collected data of a different kind from that which is normally published as an International Standard, for example "state of the art".

IEC TR 61282-9, which is a Technical Report, has been prepared by subcommittee 86C: Fibre optic systems and active devices, of IEC technical committee 86: Fibre optics.

This second edition cancels and replaces the first edition published in 2006.

This second edition includes the following significant technical changes with respect to the previous edition:

a) much of the theory has been condensed – focusing only on content that is needed to explain the test method;
b) symbols have been removed, but abbreviations are retained;

c) the material in the Clause 5 has been significantly reduced in an effort to avoid repeating what is already in the actual International Standards. Instead, the focus is on explaining the International Standards;

d) measurement methods that are not found in International Standards have been removed;

e) there are significant corrections to the modulation phase shift method, particularly in regard to the Mueller set technique;

f) there are significant corrections to the polarization phase shift method;

g) the proof of the GINTY interferometric method is presented. This proof also extends to the Fixed Analyser Cosine transfer technique;

h) another Fixed Analyser method is suggested. This is based on the proof of the GINTY method and is called "spectral differentiation method";

i) Clause 6 has been renamed "Limitations" and refocused on the limitations of the test methods. This Technical Report is not intended to be an engineering manual;

j) the annexes have been removed;

k) the bibliography has been much reduced in size;

l) the introduction has been expanded to include some information on system impairments.

The text of this Technical Report is based on the following documents:

Enquiry draft	Report on voting
86C/1342/DTR	86C/1366/RVC

Full information on the voting for the approval of this Technical Report can be found in the report on voting indicated in the above table.

This publication has been drafted in accordance with the ISO/IEC Directives, Part 2.

A list of all parts in the IEC 61282 series, published under the general title *Fibre optic communication system design guides*, can be found on the IEC website.

The committee has decided that the contents of this publication will remain unchanged until the stability date indicated on the IEC website under "http://webstore.iec.ch" in the data related to the specific publication. At this date, the publication will be

- reconfirmed,
- withdrawn,
- replaced by a revised edition, or
- amended.

A bilingual version of this publication may be issued at a later date.

IMPORTANT – The 'colour inside' logo on the cover page of this publication indicates that it contains colours which are considered to be useful for the correct understanding of its contents. Users should therefore print this document using a colour printer.

INTRODUCTION

This Technical Report is complementary to the International Standards describing PMD procedures (IEC 60793-1-48, IEC 61280-4-4, IEC 61290-11-1, IEC 61290-11-2 and IEC 61300-3-32) and other design guides on PMD (IEC 61282-3 and IEC 61292-5), as well as ITU-T Recommendation G.650.2.

The system power penalty associated with PMD varies depending on transmission format and bit rate. It also varies with optical frequency and state of polarization (SOP) of the light source. At the output of a link, the signal can shift from a maximum delay to a minimum delay as a result of using different SOPs at the source. The difference in these delays is called the differential group delay (DGD), which is associated with two extremes of input SOP. At these extremes, a signal in the form of a single pulse appears shifted up or down by half the DGD, about a midpoint, at the output. At intermediate SOPs, the single pulse appears as a weighted total of two pulses at the output, one shifted up by half the DGD and one shifted down by half the DGD. This weighted total of two shifted pulses is what causes signal distortion.

The system power penalty is partly defined in terms of a maximum allowed bit error rate and a minimum received power. In the absence of distortion, there is a minimum received power that will produce the maximum allowed bit error rate. In the presence of distortion, the received power should be increased to produce the maximum bit error rate. The magnitude of the required increase of received power is the power penalty of the distortion.

The term PMD is used to describe two distinctly different ideas.

One idea is associated with the signal distortion induced by transmission media for which the output SOP varies with optical frequency. This is the fundamental source of signal distortion.

The other idea is that of a number (value) associated with the measurement of a single-mode fibre transmission link or element of that link. There are several measurement methods with different strengths and capabilities. They are all based on quantifying the magnitude of possible variation in output SOP with optical frequency. The objective of this Technical Report is to explain the commonality of the different methods.

The DGD at the source's optical frequency is what controls the maximum penalty across all possible SOPs. However, in most links, the DGD varies randomly across optical frequency and time. The PMD value associated with measurements, and which is specified, is a statistical metric that describes the DGD distribution. There are two main metrics, linear average and root-mean square (RMS), that exist in the literature and in the measurement methods. For most situations, one metric can be calculated from the other using a conversion formula. The reason for the dual metrics is an accident of history. If history could be corrected, the RMS definition would be the most suitable.

For the non-return to zero transmission format, DGD equal to 0,3 of the bit period yields approximately 1 dB maximum penalty. Because DGD varies randomly, a rule of thumb emerged in the system standardization groups: keep PMD less than 0,1 of the bit period for less than 1 dB penalty. This assumes that DGD larger than three times the PMD, and that the source output SOP produces the worst case distortion, is not very likely. For 10 Gbit/s non-return to zero, this rule yields a design rule: keep the link PMD less than 10 ps. ITU-T G.sup.39 [1][1] has more information on the relationship of PMD and system penalties.

---

1 Numbers in square brackets refer to the Bibliography.

FIBRE OPTIC COMMUNICATION SYSTEM DESIGN GUIDES –

Part 9: Guidance on polarization mode dispersion measurements and theory

1 Scope

This part of IEC 61282, which is a Technical Report, describes effects and theory of polarization mode dispersion (PMD) and provides guidance on PMD measurements.

2 Normative references

The following documents, in whole or in part, are normatively referenced in this document and are indispensable for its application. For dated references, only the edition cited applies. For undated references, the latest edition of the referenced document (including any amendments) applies.

IEC 60793-1-48, *Optical fibres – Part 1-48: Measurement methods and test procedures – Polarization mode dispersion*

IEC 61280-4-4, *Fibre optic communication subsystem test procedures – Part 4-4: Cable plants and links – Polarization mode dispersion measurement for installed links*

IEC 61290-11-1, *Optical amplifier – Test methods – Part 11-1: Polarization mode dispersion parameter – Jones matrix eigenanalysis (JME)*

IEC 61290-11-2, *Optical amplifier – Test methods – Part 11-1: Polarization mode dispersion parameter – Poincaré sphere analysis method*

IEC 61300-3-32, *Fibre optic interconnecting devices and passive components – Basic tests and measurement procedures – Part 3-32: Examinations and measurements – Polarization mode dispersion measurement for passive optical components*

3 Terms, definitions, and abbreviations

3.1 Terms and definitions

For the purposes of this document, the following terms and definitions apply.

3.1.1
PMD phenomenon
polarization mode dispersion phenomenon
signal of fibre-optic transmission signal induced by variation in the signal output state of polarization with optical frequency

Note 1 to entry: PMD can limit the bit rate-length product of digital systems.

3.1.2
PMD value
polarization mode dispersion value
magnitude of polarization mode dispersion phenomenon associated with a single-mode fibre, optical component and sub-system, or installed link

Note 1 to entry: The polarization mode dispersion value is usually expressed in ps.

3.2 Abbreviations

CFT cosine Fourier transform
DGD differential group delay
DOP degree of polarization
EC extrema counting
FA fixed analyser
FT Fourier transform
GINTY general interferometric method
JME Jones matrix eigenanalysis
MPS modulation phase shift
OTDR optical time domain reflectometer
PDL polarization dependent loss
PDV polarization dispersion vector
PMD polarization mode dispersion
PPS polarization phase shift
PSA Poincaré sphere analysis
PSP principal state of polarization
SMF single-mode fibre
SOP state of polarization
SPE Stokes parameter evaluation
TINTY traditional interferometric method
WSOSA wavelength scanning OTDR and SOP analysis method

4 Theoretical framework

4.1 Limitations and outline

The theory presented in Clause 4 does not include the effects of polarization dependent loss or gain, or nonlinear effects. See 6.3 for information on polarization dependent loss.

The outline for Clause 4 is

- optical field and state of polarization;
- measurement of SOP, Stokes vector, and rotation;
- first order polarization mode dispersion;
- birefringence vector, concatenations, and mode coupling;
- the statistics of PMD and second order PMD.

4.2 Optical field and state of polarization

This subclause is intended to show the linkage between the propagation of an optical field in a single-mode fibre (SMF) and the transmission signal state of polarization (SOP). This information is fundamental to the PMD phenomena because variation in output SOP with optical frequency is the distortion inducing mechanism.

The solution of the wave equation has degenerated eigenvalues. This means that even the fundamental solution is degenerated. A SMF supports a pair of polarization modes for a monochromatic light source. In particular, the lowest order mode, namely the fundamental

mode HE_{11} (LP_{01}) can be defined to have its transverse electric field predominately along the x-direction; the orthogonal polarization is an independent mode, as shown in Figure 1.

In a lossless SMF, the electric field vector of a monochromatic electromagnetic wave propagating along the z-direction can be described by a linear superposition of these two modes in the x-y transverse plane as shown in Equation (1) and in Figure 1.

$$E = \left\{\left[j_x \exp\left(i\beta_x z\right)\right] + \left[j_y \exp\left(\beta_y z\right)\right]\right\}\exp\left(-i\varpi t\right)$$

$$= \left[j_x \exp\left(-\Delta\beta z/2\right) + j_y \exp\left(i\Delta\beta z/2\right)\right]\exp\left[-i\left(\varpi t - \overline{\beta} z\right)\right] \quad (1)$$

where

j_x and j_y are complex coefficients describing the amplitude and phase of the x/y initial SOPs;

$E_x(x,y)$ and $E_y(x,y)$ are the spatial variation (in the x-y transverse plane) of the E vector of the PM along the x/y-direction (see Figure 1);

β_x and β_y are the propagation constants (also called effective index or wavenumber) of the PM along the x/y-directions with the index of refraction n_x/n_y. Using $i = x$ or y, $\beta_i = k \cdot n_i$. The index of refraction has a dependence on frequency ϖ, frequency ν, or wavelength λ;

$\Delta\beta$ is the difference of β_x and β_y;

$\overline{\beta}$ is the average of βx and βy;

k is the propagation constant with the wavelength λ in vacuum ($= 2\pi\nu/c = 2\pi/\lambda = \omega/c$);

ν is the frequency in s^{-1} or Hz;

ϖ is the angular frequency in rad/s (the bar indicates absolute frequency rather than deviation from some particular value);

c is the speed of light in vacuum (299792458 m/s);

Δ' is the birefringence coefficient (s/m), $= \Delta n/c$

z is the distance (m) in the DUT along the optical axis (axis of propagation); $z = L$ at the output of the DUT with length L.

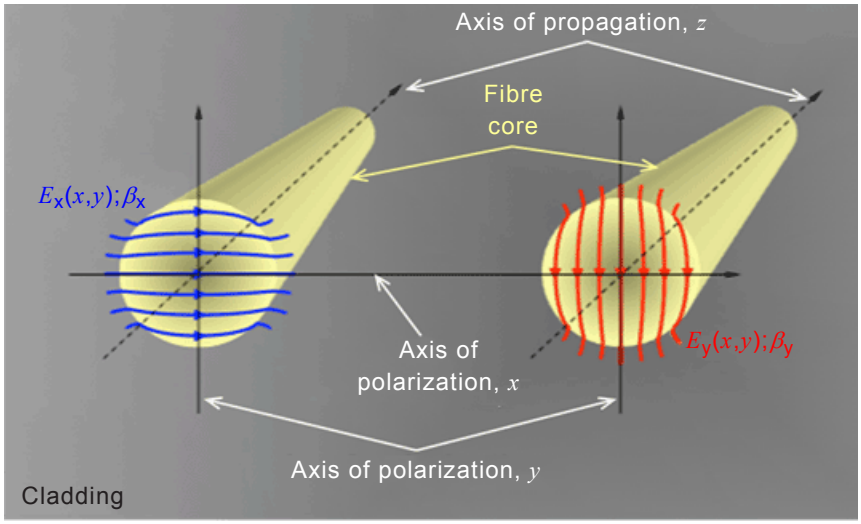

Figure 1 – Two electric field vector polarizations of the HE_{11} mode in a SMF

The complex pair, $\left[j_x \exp(-i\Delta\beta z/2), j_y \exp(i\Delta\beta z/2)\right]$, describes the SOP defined in the x-y plane of the wave propagating along the z-direction. This pair can be considered as a vector, and is often called a Jones vector.

In the case where the transmission media is an ideal SMF with perfect circular symmetry, $\beta_y = \beta_x$,

- the two polarization modes are degenerate (when two solutions have the same eigenvalue, they are said to be degenerate);
- any wave with a defined input SOP will propagate unchanged along the z-direction throughout the output of the SMF.

However, in a practical SMF, the circular symmetry is broken by imperfections produced by the fabrication process, cabling, field installation/use or the installation environment:

- $\beta_y \neq \beta_x$, implying a phase difference, an index-of-refraction difference Δn, and a phase-velocity difference between the two PMs;
- the degeneracy of the two polarization modes is lifted;
- the SOP of an input wave will change along the z-direction throughout the output of the SMF.

The difference between β_y and β_x, namely $\Delta\beta$, is called the phase birefringence or simply the birefringence and has units of inverse length (m^{-1}). Birefringence may also be referred to as the index difference, Δn, or as the birefringence coefficient, the difference divided by length. Birefringence coefficient values typically vary between 0,25 fs/m and 2,5 fs/m in commonly available SMFs.

As the SOPs travel through the fibre, they will return to the initial state at positions that are increments of $2\pi/\Delta\beta$. At these positions, the two field components will beat. The difference between these positions is called the beat length.

Birefringence can be induced by a number of factors such as core non-circularity or asymmetric stresses that can be induced by bends, twist, and compression. These factors change over the length of the fibre and can change over time due to changes in configuration, or temperature. These factors will also vary with optical frequency. Equation (1) is also defined with an arbitrary coordinate system that will not generally correspond to the laboratory or field test equipment coordinate system. The mapping of the input SOP to the output SOP

over a particular length and optical frequency, L and ϖ_0, is represented with the Jones matrix, T, and the input and output Jones vectors, $\vec{j}_{IN}$ and $\vec{j}_0$, as:

$$\vec{j}_0 = T\vec{j}_{IN} \tag{2}$$

where

$$T = V_T S_T V_T^{\uparrow} \tag{3}$$

$$S_T = \begin{bmatrix} \exp(-i\xi_T/2) & 0 \\ 0 & \exp(i\xi_T/2) \end{bmatrix} \tag{4}$$

$$V_T = \begin{bmatrix} \cos\theta_T \exp(-i\mu_T/2) & -\sin\theta_T \exp(-i\mu_T/2) \\ \sin\theta_T \exp(i\mu_T/2) & \cos\theta_T \exp(i\mu_T/2) \end{bmatrix} = S(i\mu_T/2)R(\theta_T) \tag{5}$$

NOTE 1 The subscript T is used to distinguish the matrix parameters from similar parameters used later.

The main operation of Equation (3), corresponding to Equation (1), is found in the matrix, S_T. Pre and post-multiplying by V_T and $V_T^{\uparrow}$ is a change of coordinates. The notation $V^{\uparrow}$ indicates the transpose conjugate for matrices and vectors.

The diagonal expressions in Equation (4) are intended to show the connection to Equation (1). Equation (1), however, is only applicable locally, while Equation (3) is used to indicate change over the entire transmission media. There is another expression that uses $\gamma_T = \xi_T/2$ that is found in ITU-T Recommendation G.650.2. On the Poincaré sphere, the action of Equation (4) is a rotation of γ_T from an input SOP to an output SOP. When equations are found in both documents, the γ_T notation will be used.

Unit Jones vectors, which are one way to represent SOPs, can be specified with a *(θ,μ)* pair as:

$$\vec{j} = \begin{bmatrix} \cos\theta \exp(-i\mu/2) \\ \sin\theta \exp(i\mu/2) \end{bmatrix} \tag{6}$$

The Jones matrix, T, is unitary in that $T^{\uparrow}T = I$, the identity matrix. The columns of V_T are the eigenvectors, and the diagonal elements of S_T are the eigenvalues. When the input Jones vector is equal to either of the eigenvectors, the output SOP is the same as the input SOP because the SOP is not affected by a multiplication by a constant. These states are sometimes called the eigenstates.

NOTE 2 All the parameters of T can change with optical frequency, as well as with changes caused by fibre movement over time or temperature change.

4.3 SOP measurements, Stokes vectors, and Poincaré sphere rotations

The SOP is usually measured with a polarimeter, which yields a Stokes vector. The measurement is actually done with a series of power measurement differences through various states of a polarizer/analyser.

An ideal polarizer may be defined as:

$$Pol(\theta_P, \mu_P) = V_{Pol}\begin{bmatrix}1 & 0\\ 0 & 0\end{bmatrix}V_{Pol}^{\uparrow} = \begin{bmatrix}\cos^2\theta_P & \frac{1}{2}\sin 2\theta_P \exp(-i\mu_P)\\ \frac{1}{2}\sin 2\theta_P \exp(i\mu_P) & \sin^2\theta_P\end{bmatrix} \quad (7)$$

where V_{Pol} is of the same form as Equation (5), but with different parameters.

For a given Jones vector, the power through the polarizer is:

$$P(\theta_P, \mu_P) = \vec{j}^{\uparrow} Pol^{\uparrow}(\theta_P, \mu_P) Pol(\theta_P, \mu_P)\vec{j} \quad (8)$$

The measured Stokes vector is given as:

$$\vec{S} = \begin{bmatrix}P(0,0) + P(\pi/2,0)\\ P(0,0) - P(\pi/2,0)\\ P(\pi/4,0) - P(-\pi/4,0)\\ P(\pi/4,\pi/2) - P(\pi/4,-\pi/2)\end{bmatrix} \text{ indexed with } j = 0,1,2,3 \quad (9)$$

The normalized Stokes vector is designated with a small $\vec{s}$ and has three elements indexed: 1, 2, and 3. The normalized Stokes vector elements are the measured Stokes vector element values with the same index, divided by S_0. The normalized Stokes vector has a length of one.

SOPs where s_3 is zero are linear states. When s_3 is nonzero but with absolute value less than one, the polarization is elliptical. When s_3 is ±1, the polarization is circular.

NOTE 1 In the rest of this Technical Report, the normalized Stokes vector will be referred to simply as the Stokes vector.

The degree of polarization (DOP) is normally expressed as a per cent and is equal to $100 \cdot S_0 / P$, where P is the power without the polarizer.

A unit Jones vector can be represented either as an *x/y* pair or as Equation (6). The relationship of the normalized Stokes vector to the Jones vector is given as:

$$\vec{s} = \begin{bmatrix}xx^* - yy^*\\ xy^* + yx^*\\ i(xy^* - yx^*)\end{bmatrix} = \begin{bmatrix}\cos 2\theta\\ \sin 2\theta \cos\mu\\ \sin 2\theta \sin\mu\end{bmatrix} \quad (10)$$

There is an ambiguity in trying to calculate the Jones vector from the Stokes vector. One must assume something like $0<\theta<\pi$. This is due to the fact that the Stokes vector is not affected by multiplying the Jones vector by any unit complex number (a number, c, for which $cc^* = 1$), including ±1. This can be called a one π ambiguity. This property is one reason to think of the Stokes vector as the primary definition of the SOP: the SOP is not changed when either of the eigenstates are used as inputs, but the output Jones vector is multiplied by $\exp(\pm i\xi_T/2)$.

Unit three term vectors can be represented on a sphere. In the case of Stokes vectors, the sphere is called the Poincaré sphere.

Examination of the rightmost expression of Equation (10) and the different parts of Equations (3), (4) and (5) shows that the action of T is consistent with the following right-hand-rule rotations applied to the input Stokes vector that corresponds to the input Jones vector:

a) anti-rotation of μ_T about the (1,0,0) vector, which describes a linear SOP;

b) anti-rotation of $2\theta_T$ about the (0,0,1) vector, which describes a circular SOP;

c) rotation of ξ_T (= $2\gamma_T$) about the (1,0,0) vector;

d) rotation of $2\theta_T$ about the (0,0,1) vector;

e) rotation of μ_T about the (1,0,0) vector.

These steps can be combined into a single rotation, from input Stokes vector to output Stokes vector, as:

$$\vec{s}_0 = R_T \vec{s}_{IN} \tag{11}$$

where

$$R_T = \vec{y}\vec{y}^T(1-\cos\xi_T) + I\cos\xi_T + \left[\vec{y}\times\right]\sin\xi_T \tag{12}$$

where $\vec{y}^T$ is the transpose of $\vec{y}$, I is the identity matrix, and $\left[\vec{y}\times\right]$ is the cross product operator, $\begin{bmatrix} 0 & -y_3 & y_2 \\ y_3 & 0 & -y_1 \\ -y_2 & y_1 & 0 \end{bmatrix}$.

This is a rotation of ξ_T about the rotation vector, $\vec{y}$. The rotation vector is found by converting the first column of V_T to a Stokes vector. Figure 2 illustrates a rotation on the Poincaré sphere. This is a 2π rotation about the (1,0,0) axis.

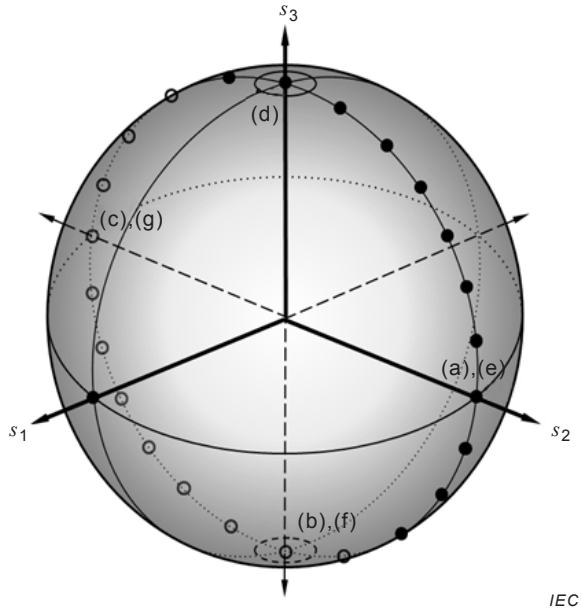

Figure 2 – A rotation on the Poincaré sphere

The T matrix can now be written in a simplified form:

$$T = \begin{bmatrix} \cos\gamma_T - iy_1\sin\gamma_T & -(y_3 + iy_2)\sin\gamma_T \\ (y_3 - iy_2)\sin\gamma_T & \cos\gamma_T + iy_1\sin\gamma_T \end{bmatrix}$$

$$= \cos\gamma_T I - i\sin\gamma_T \begin{bmatrix} y_1 & y_2 - iy_3 \\ y_2 + iy_3 & -y_1 \end{bmatrix} \quad (13)$$

NOTE 2 The form of this equation re-emerges in Equation (20), in which it is pointed out that the rightmost matrix is the weighted sum of Pauli matrices.

4.4 First order polarization mode dispersion

First order PMD is induced by the variance in the output Jones vector with optical frequency. This is the same as the variance of the output Stokes vector with frequency, which is one way to measure it, but the signal distortion must be understood in terms of the Jones calculus. To distinguish the variance of SOP with optical frequency from the input-to-output Jones matrix of the prior clauses, the frequency transfer matrix is designated with $J(\omega)$ as

$$\vec{j}_{OUT}(\omega) = J(\omega)\vec{j}_0 = V_J \begin{bmatrix} \exp(-i\Delta\tau\omega/2) & 0 \\ 0 & \exp(i\Delta\tau\omega/2) \end{bmatrix} V_J^{\uparrow} \vec{j}_0 \quad (14)$$

where

V_J is the same form as Equation (5);

ω is deviation from the particular frequency, ϖ_0;

$\vec{j}_0$ is the output SOP at that frequency;

$\vec{j}_{OUT}(\omega)$ is the output Jones vector at the frequency, $\varpi_0+\omega$;

$\Delta\tau$ is the differential group delay (DGD).

The exponent of the ratio of eigenvalues of J yields $\Delta\tau\Delta\omega$ for a finite frequency increment.

The action of $J(\omega)$ is a rotation on the Poincaré sphere from the output Stokes vector at ϖ_0 to the Stokes vector at $\varpi_0+ \omega$. The rotation angle is $\Delta\tau\omega$, and the rotation vector is formed by transforming the first column of V_J into a Stokes vector. This rotation vector is called the principal state of polarization (PSP) and is later designated as a vector, $\vec{p}$.

The distortion can be understood by considering the Fourier transform of the signal field, $H(\omega)$ and its inverse transform, $h(t)$. Time shifting of the inverse transform is given as transform pair as:

$$\exp(it_0\omega)H(\omega) \Leftrightarrow \frac{1}{2\pi} h(t - t_0) \quad (15)$$

The output Jones vector in the time domain is therefore given as:

$$\vec{j}_{OUT}(t) = \frac{1}{2\pi} V_J \begin{bmatrix} h(t - \Delta\tau/2) & 0 \\ 0 & h(t + \Delta\tau/2) \end{bmatrix} V_J^{\uparrow} \vec{j}_0 \quad (16)$$

The output power is the conjugate transpose of the output Jones vector times itself. When V_J is the identity matrix and the elements of $\vec{j}_0$ are both equal to $\sqrt{2}$, the output pulse is the sum of squares of two field pulses separated by $\Delta\tau$. This represents a worst case for distortion within the first order formulation.

When $\vec{j}_0$ is equal to either column of V_J, there is no distortion, but the signal is shifted in the time domain by $\pm\Delta\tau/2$. At intermediate polarization states, the output pulse is the total of two time shifted pulses of different magnitudes. In the worst case, the magnitudes are equal.

In the Stokes formulation, the action of Equation (14) is a rotation, R_J, with rotation angle, $\Delta\tau\omega$, about rotation vector, $\vec{p}$. The rotation vector is found by converting the first column of V_J to a Stokes vector. This rotation vector is also called the fast PSP, because when $\vec{s}_0$ is equal to this vector, there is, to the first order, no change in the output Stokes vector with frequency. Since it is aligned with $-i\Delta\tau\omega/2$, it is the early arriving, or fast, part of the signal.

For completeness, R_J is of the form of Equation (12), but with different parameters, and the relationship of the output Stokes vector as a function of frequency is:

$$\vec{s}_{OUT}(\omega) = R_J(\omega)\vec{s}_0 \tag{17}$$

Two important objects in the PMD literature are the polarization dispersion vector (PDV), designated as $\vec{\Omega}$ and the frequency transfer function differential operator, a matrix designated as D. These are defined as the following, considering that all parameters of both RT and T are functions of frequency:

$$\frac{d\vec{s}_{OUT}(\omega)}{d\omega}\Big|_0 = \frac{dR_T(\omega)}{d\omega}\Big|_0 R_T(0)^T\vec{s}_0 = \left[\vec{\Omega}\times\right]\vec{s}_0 = \left[\left(\Delta\vec{\tau}\right)\times\right]\vec{s}_0 \tag{18}$$

When the output Stokes vector at ϖ_0, designated as $\vec{s}_0$, is aligned with the PSP or PDV, there is no change in the output Stokes vector with respect to frequency, to the first order.

$$\frac{d\vec{j}_{Out}(\omega)}{d\omega}\Big|_0 = D\vec{j}_0 = \frac{dT(\omega)}{d\omega}\Big|_0 T^{-1}(0)\vec{j}_0 = \frac{dJ(\omega)}{d\omega}\Big|_0\vec{j}_0 = V_J\begin{bmatrix} -i\Delta\tau/2 & 0 \\ 0 & i\Delta\tau/2 \end{bmatrix}V_J^{\uparrow}\vec{j}_0$$

$$= -i\frac{\Delta\tau}{2}\begin{bmatrix} p_1 & p_2 - ip_3 \\ p_2 + ip_3 & -p_1 \end{bmatrix}\vec{j}_0 \tag{19}$$

The matrix expression in the last term is the weighted sum of the three Pauli operators:

$$\sigma_1 = \begin{bmatrix} 1 & 0 \\ 0 & -1 \end{bmatrix}\quad \sigma_2 = \begin{bmatrix} 0 & 1 \\ 1 & 0 \end{bmatrix}\quad \sigma_3 = \begin{bmatrix} 0 & -i \\ i & 0 \end{bmatrix} \tag{20}$$

The eigenvalues of D are $\pm i\Delta\tau/2$.

Expansion of the expressions containing the parameters of T shows the following:

- the equations are consistent;
- a differential equation that links the parameters and derivative of T to the PDV emerges.

$$\vec{\Omega} = 2\frac{d\gamma_T}{d\varpi}\vec{y} + \sin 2\gamma_T\frac{d\vec{y}}{d\varpi} + 2\sin^2\gamma_T\left(\vec{y}\times\frac{d\vec{y}}{d\varpi}\right) \tag{21}$$

Given the PDV as a function of optical frequency and suitable boundary conditions, the parameters of T, hence T can be solved using numerical techniques. This was important in simulating the interferometric measurement method.

First order PMD means that the exponent of the diagonal matrix in Equation (14) is linear in frequency. In reality, there are limitations in the first order projections because the PSP and DGD actually vary with frequency in most (long) transmission media.

4.5 Birefringence vector, concatenations, and mode coupling

4.4 indicated that the important parameters, the PSP and DGD, also vary with optical frequency. 4.5 will give some background as to why this is so.

The birefringence vector is defined by replacing the frequency (ω) derivatives with length (z) derivatives in Equations (18) and (21). Also, replace the symbol for the PDV with the symbol for the birefringence vector. The evolution of the output Stokes vector through a length of transmission media can be calculated from the modified Equation (18) and a set of assumptions about the birefringence vector. These assumptions can include factors such as twist, which induces circular birefringence, bend, lateral load, and spin.

A simple birefringent element can be defined from Equations (3) through (5) with the following:

$$\text{Set } \xi_T = \varpi z \Delta' \text{ and } \mu_T = 0 \tag{22}$$

where Δ' is the birefringence coefficient (s/m).

A concatenation of a number of randomly rotated simple birefringent elements will induce mode coupling that varies with optical frequency. As a result, depending on the number and length of such elements, the output SOPs no longer follow simple rotations with frequency, and the PDV becomes random. Figure 3 shows an example.

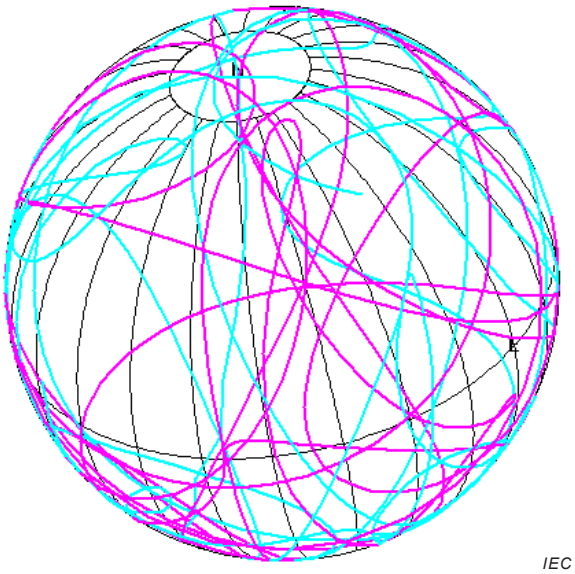

Figure 3 – Strong mode coupling – Frequency evolution of the SOP

Negligible mode coupling would display a less complicated evolution, such as what is shown in Figure 2. However, there is no firm boundary between the different regimes.

The concatenation of randomly rotated simple elements is not a complete model for optical fibre. The PMD behaviour of optical fibre and cable is in the realm of strong random mode coupling. Most optical fibre is manufactured using a spinning technique to deliberately introduce strong mode coupling.

Consequences of mode coupling include:

- the connection between the birefringence vector and the PDV is lost. The birefringence vector is a local phenomenon, while the PDV is a result of transmission over the whole of the media;
- DGD varies randomly with frequency;
- the PSP varies randomly with frequency;
- the first order PMD model is an approximation that is only applicable for a narrow frequency interval;
- depending on the measurement type, frequency domain or time domain, the sampling density and/or extent must take into account the random nature of the phenomenon;
- the PMD value that is reported must be derived from a statistical calculation;
- PMD increases with the square root of length, leading to the definition of the PMD coefficient as the PMD measured value divided by square root of the transmission length;
- there is a phenomenon called second order PMD, which is a measure of how the DGD and PSP vary with frequency;
- third- and higher-order PMD may have an effect on the distortion at very high bit rates or under particular transmission formats but have not been studied.

4.6 The statistics of PMD and second order PMD

This subclause assumes the transmission media is in the random mode coupling regime.

A first consequence of random mode coupling is that the three elements of the PDV become independently distributed Gaussian random variables if the frequency points are far enough apart. The average of these distributions is zero, and there is a common standard deviation, σ. The DGD, $\Delta\tau$, is the square root of the sum of squares of the three elements. This means that the distribution of DGD values is ideally Maxwellian, with probability density function given as Equation (23).

$$f_{Maxwell}(\Delta\tau) = \sqrt{\frac{2}{\pi}} \frac{\Delta\tau^2}{\sigma^3} \exp\left(-\frac{\Delta\tau^2}{2\sigma^2}\right) \tag{23}$$

The PMD value that is reported from measurements is derived from one of two main statistical calculations:

- root mean square (RMS) equals square root of average of squares of DGD values across frequencies;
- linear average equals a simple average of DGD values across frequencies

Exceptions to these statistics may be found for some components for which the negligible mode coupling regime applies. In these cases, the maximum DGD can be reported. A PMD can still be reported, but the Maxwell approximation does not hold.

The RMS statistic is the most "natural" for PMD (see Equation (24)), but the linear average was standardized for fibre and cabled fibre measurements before PMD was more completely understood. This is of particular importance for the interferometric measurement methods, where the value reported is equivalent to the RMS statistic.

The RMS value is expressed with the expected value operator as $\left\langle \Delta\tau^2 \right\rangle^{1/2}$. The linear average is expressed as $\left\langle \Delta\tau \right\rangle$. Depending on which statistic is reported, the σ parameter found in Equation (23) can be replaced with either the expression in Equation (24) for RMS or with Equation (25) for linear average.

$$\sigma^2 = \frac{1}{3}\left\langle \Delta\tau^2 \right\rangle \tag{24}$$

$$\sigma = \left\langle \tau \right\rangle \sqrt{\frac{\pi}{8}} \tag{25}$$

From these equations, it can be deduced that the RMS value is approximately $\sqrt{\frac{3\pi}{8}}$ larger than the linear average.

Figures 4 and 5 illustrate the random DGD both as a plot vs. wavelength (frequency) and as a histogram.

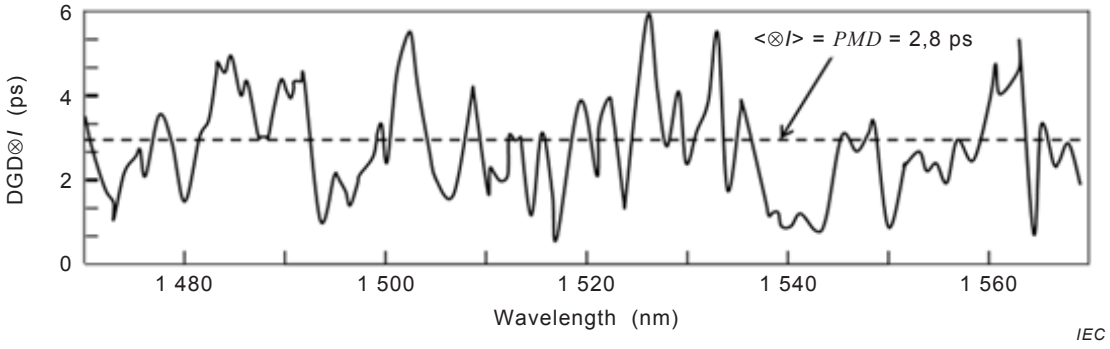

Figure 4 – Random DGD variation vs. wavelength

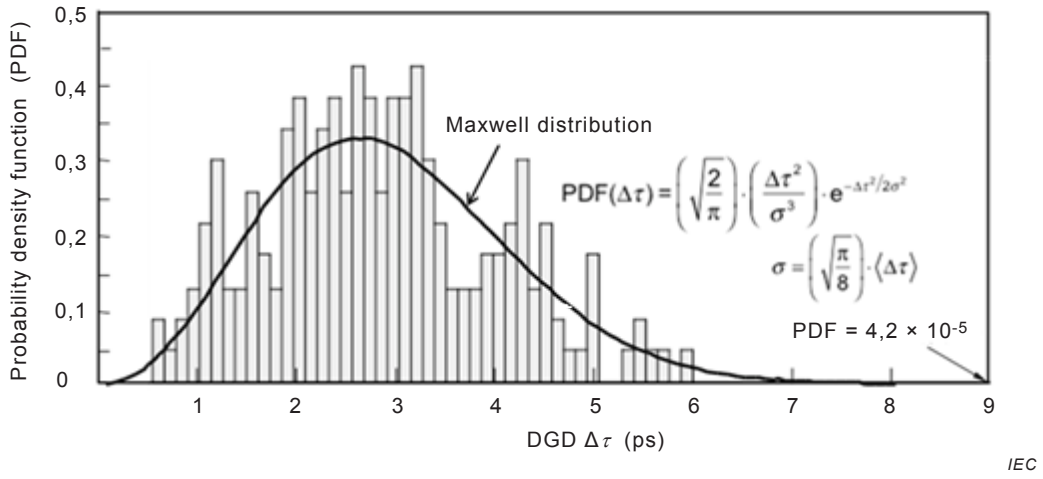

Figure 5 – Histogram of DGD values from Figure 4

For the frequency domain measurements, there is a scan of frequencies from ϖ_1 to ϖ_2 with an increment of $\Delta\omega$. The extent and sampling density needed depend on the expected PMD of the transmission media being measured.

NOTE For time domain measurements, the time increment is inversely proportional to the frequency extent and the time extent is inversely proportional to the frequency increment.

Guidance on the frequency extent can be derived from the fixed analyser measurement method (see 5.5). This method relates the RMS PMD to the number of extrema, N_e, counted over the frequency scan as

$$\left\langle \Delta\tau^2 \right\rangle^{1/2} \approx \sqrt{\frac{3\pi}{8}} \frac{\pi N_e}{\varpi_2 - \varpi_1} \tag{26}$$

As the number of extrema increases, the reproducibility of the PMD measurements improves. One way to increase the number of extrema is to measure across a wider frequency interval. Equation (27), from Gisin [2] relates the frequency extent to the uncertainty (one standard deviation) of the measurement compared to the result one might obtain with a very large (approaching infinity) frequency extent.

$$\left\langle \Delta\tau^2 \right\rangle^{1/2} \approx \left\langle \Delta\tau^2 \right\rangle_\infty^{1/2} \left(1 \pm \frac{0{,}9}{\sqrt{\left\langle \Delta\tau^2 \right\rangle_\infty^{1/2} (\varpi_2 - \varpi_1)}} \right) \tag{27}$$

If the frequency extent is 16 THz, corresponding to 129 nm around 1 550 nm, and the PMD is 1 ps, the measurement uncertainty is about 9 %. However, if the wavelength range were increased from 1 310 nm to 1 625 nm, the uncertainty would be reduced to around ±5 %.

One reason for the uncertainty situation is second order PMD, which is expressed as the frequency derivative of the PDV, i.e., $\vec{\Omega}_\omega$. It is related to the PMD according to the following

$$\left\langle \vec{\Omega} \cdot \vec{\Omega} \right\rangle = \left\langle \left| \vec{\Omega} \right|^2 \right\rangle = \left\langle \Delta\tau^2 \right\rangle \tag{28}$$

$$\left\langle \left| \vec{\Omega}_\omega \right|^2 \right\rangle = \left\langle (\Delta\tau_\omega)^2 \right\rangle + \left\langle \Delta\tau^2 \left| \vec{p}_\omega \right|^2 \right\rangle \tag{29}$$

$$\left\langle \left| \vec{\Omega}_\omega \right|^2 \right\rangle = \frac{1}{3} \left\langle \left| \vec{\Omega} \right|^2 \right\rangle^2 \tag{30}$$

$$\left\langle (\Delta\tau_\omega)^2 \right\rangle = \frac{1}{27} \left\langle \left| \vec{\Omega} \right|^2 \right\rangle^2 \tag{31}$$

$$\left\langle \Delta\tau^2 \left| \vec{p}_\omega \right|^2 \right\rangle = \left\langle \left| \vec{\Omega}_{\perp\omega} \right|^2 \right\rangle = \frac{8}{27} \left\langle \left| \vec{\Omega} \right|^2 \right\rangle^2 \tag{32}$$

Second order PMD RMS (square root of Equation (30)) increases as the square of PMD, and the result is dominated by the part associated with the PSP (Equation (32)). On the other hand, for very low PMD, a measurement at a single frequency might not be much different from measurements across a range that is practical.

Another outcome of the uncertainty is that optical fibre cable is specified statistically using a parameter called the link design value or PMDQ. IEC TR 61282-3 [9] explains this statistic more completely, but it is an upper confidence limit, at 99,99 % probability, on the concatenated PMD coefficient of 20 cables. The statistic takes both average and variance of the PMD distribution into account. The variance includes measurement uncertainty, so the statistical specification is a primary way of managing measurement uncertainty.

4.7 Managing time

The output SOP can be modified by factors other than optical frequency. These factors can change with time. Factors include:

- Temperature

  Even for buried cabling, small temperature changes over long times can produce changes in the DGD that are apparently random when the times between measurements are sufficiently long.

- Vibration

  Some aerial lines have high frequency variations. Another source could be railroads or highways.

- Bending variation

  This can be caused by winds.

- Rewinding the cabled fibre

- Uncontrolled changes in the input SOP

  This is important for active system monitoring.

Changes in these factors over the time of measurement can result in errors, depending on the measurement method. Except for uncontrolled changes in the input SOP, the main effects of these sources of variation are changes in mode coupling.

For frequency domain measurements, at least a part of the output SOP shall be measured at either a pair of frequencies, otherwise a means of evaluating the frequency derivative shall be provided in order to obtain an estimate of the DGD. The measurement time for such a pair should be small in comparison to the factor variation rate, e.g., 1 ms for vibration noise in the range of 50 Hz to 60 Hz.

When such a small interval is not practical, there are alternatives:

- wait until the disruptions are not changing, e.g., the wind stops, or the train is gone;
- use a time domain, interferometric measurement.

The slow variation with small temperature changes produces a different random DGD curve vs. optical frequency at one time vs. another. This gives rise to the term "instantaneous DGD".

Depending on the type of physical perturbations, the statistics of the DGD across time at a given frequency are similar to the statistics of the DGD across frequencies at a single time. This is an aspect that can be exploited in system monitoring.

Verification of the stability of the output Stokes vector as a function of time is a prudent thing to do, particularly for measurement of installed links. There is, however, no formal requirement to do this check or a standardized criterion for "stability".

5 Measurement methods

5.1 General

There are several international publications that describe some common measurement methods. Each such publication is normative to the products to which the publication applies. The product categories and normative test publications are:

- optical fibre and cable: IEC 60793-1-48;

- optical amplifiers: IEC 61290-11-1 and IEC 61290-11-2 (IEC TR 61292-5 [10] for information);
- passive optical components: IEC 61300-3-32;
- installed links: IEC 61280-4-4.

These normative test procedures differ in respect to details that are especially critical to the product. For example, the amplifier documents pay particular attention to amplified spontaneous emissions. The passive component document provides some guidance on polarization dependent loss for devices with small levels of PMD and which are in the negligible mode coupling regime.

Another aspect relevant to optical components is that some components such a wavelength division multiplexing devices have multiple optical paths that require special procedures. Provisions for devices with multiple optical paths are not in the scope of this Technical Report.

Each normative test publication has one or more measurement methods. The same measurement methods appear in multiple normative publications. The intent of this Technical Report is to explain how the different measurement methods relate to the underlying theory. It is not the intent of this Technical Report to repeat the technical requirements found in the individual normative test procedures listed above. In some cases, however, some of the requirements must be repeated in order to provide background necessary for the explanation.

The methods include

- Stokes parameter evaluation (SPE):
  - Jones matrix eigenanalysis (JME);
  - Poincaré sphere analysis (PSA).
- Phase based measurements:
  - modulation phase shift (MPS);
  - polarization phase shift (PPS).
- Interferometric methods:
  - traditional interferometric method (TINTY);
  - general interferometric method (GINTY).
- Fixed analyser (FA):
  - extrema counting (EC);
  - Fourier transform (FT);
  - cosine Fourier transform (CFT).
- Wavelength scanning OTDR and SOP analysis method (WSOSA).

The main list items use common equipment and procedures, while the indented list items differ mainly in the analysis. There are some equipment modifications to the TINTY, for example, that are needed to complete the GINTY measurement, but most of the equipment needs are quite similar.

SPE, FA, and phase based measurements involve a scan of optical frequency from a lower frequency to an upper frequency at a frequency increment. For SPE and phase based measurements, the DGD is reported for each increment, and the PMD value is based on DGD statistics, either linear average or RMS.

See 4.6 for information on frequency range and increment. The different publications have requirements for the frequency increment based on a requirement that the output Stokes rotation from one frequency to the next should not exceed 180° (on the Poincaré sphere), but considering second order PMD, this limit is too large for randomly coupled transmission

media. Instead, a rule based on apparent continuity of the result should be used. In any case, the larger the PMD being measured, the smaller the increment shall be.

For FA and interferometric methods, the PMD as a whole is reported. For interferometric methods, the PMD is reported as RMS DGD value. For FA, PMD is reported as linear average DGD. Equations (24) and (25) can be used to convert either way.

Table 1 shows which test methods are defined in which International Standards. An X denotes a normative method; a Y denotes an informative method.

Table 1 – Map of test methods and International Standards

Method	SPE			Phase		Interferometric		Fixed analyser		
Standard	JME	PSA	WSOSA	MPS	PPS	TINTY	GINTY	EC	FT	CFT
60793-1-48	X	X				X	X	X	X	X
61280-4-4	X	Y	X	Y	Y	X	X		X	
61290-11-1	X									
61290-11-2		X								
61300-3-32	X	X		X	X	X	X	X	X	
NOTE While WSOSA has a separate clause, it is categorized as a Stokes Parameter Evaluation method because of the similarity to the others in this category. It is a frequency domain method that is based on differences between Stokes characteristics of adjacent frequency pairs.										

5.2 Stokes parameter evaluation

5.2.1 Equipment setup and procedure

Figure 6 shows an equipment diagram.

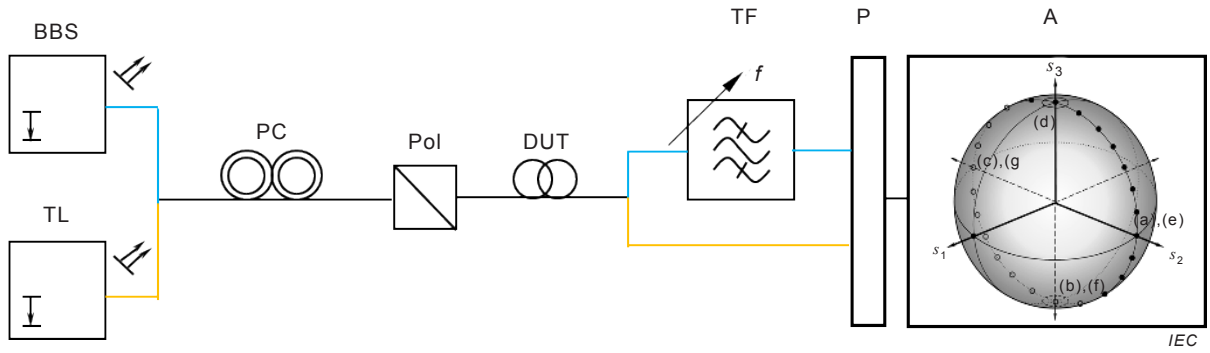

Key

BBS broadband source
TL tuneable laser
PC polarization controller
Pol polarizer (3 SOPs)
TF tunable filter
P polarimeter
A stroke parameter analyzer

Figure 6 – SPE equipment diagram

Figure 6 shows some different options:

- broadband source and tuneable filter that could be used for either PSA or JME;
- tuneable laser that could also be used for either PSA or JME.

Either the filter or tuneable laser is scanned across the frequency range, $\varpi 1$ to $\varpi 2$, in increments of $\Delta\omega$. At each frequency, the polarization controller is swept through three input linear SOPs: θ = 0, $\pi/4$, and $\pi/2$, with μ = 0 (see Equations (6) and (10)). The normalized output Stokes vectors associated with these input states are measured and called $\vec{H}$, $\vec{Q}$, and $\vec{V}$, respectively.

The rotation of the output SOP from one frequency to another is deduced using either the Jones formulation of Equation (16), or the equivalent rotation on the Poincaré sphere directly using calculations in 5.2.2 and 5.2.3. These calculation methods are exactly equivalent for DGD.

The DGD is reported for each adjacent pair of frequencies, and finally, the PMD is calculated using either the RMS or linear average of the DGD values.

5.2.2 Jones matrix eigenanalysis

This describes the calculations for a pair of frequencies, ϖ_0 and $\varpi_0+\Delta\omega$.

The output Stokes vectors are converted to complex Jones vectors: $\vec{h}$, $\vec{q}$, and $\vec{v}$ using Equations (6) and (10) for each frequency using an assumption that $\theta<\pi$.

The T matrices are calculated for each frequency. Given the following, one might think that the elements of the T matrix could be taken directly from the elements of the horizontal and vertical outputs:

$$\begin{bmatrix}\vec{h} & \vec{v}\end{bmatrix} = T\begin{bmatrix}1 & 0\\ 0 & 1\end{bmatrix} \tag{33}$$

Due to the one π ambiguity in the conversion of Stokes vectors to Jones vectors, Equation (33) is not quite a valid way of estimating T. Instead, the following ratios, which are not affected by the ambiguity, are calculated:

$$k_1 = \frac{h_x}{h_y} \quad k_2 = \frac{v_x}{v_y} \quad k_3 = \frac{q_x}{q_y} = \frac{T_{00}+T_{01}}{T_{10}+T_{11}} \quad k_4 = \frac{k_3-k_2}{k_1-k_3} = \frac{T_{10}}{T_{11}} \tag{34}$$

For the last two equations in Equation (34), the terms on the left are numbers and the terms on the far right are relationships. The T matrix estimate is now given as the following:

$$\tilde{T} = \begin{bmatrix}k_1k_4 & k_2\\ k_4 & 1\end{bmatrix} = \begin{bmatrix}h_x/v_y & v_x/v_y\\ h_y/v_y & v_y/v_y\end{bmatrix} \tag{35}$$

It is stated that the actual T matrix is equal to this estimate times an arbitrary complex constant.

The first matrix expression of Equation (35) provides a numerical estimate of T. The second matrix expression shows that the mysterious constant is $\pm v_y$. This expression results from expanding the expression for k_4. The one π ambiguity is now isolated to the sign of the matrix,

which can be arbitrary. Given a sequences of frequencies, the signs could be chosen for continuity.

NOTE Most implementations of the JME do not carry out the multiplication by $\pm v_y$. They do not need to.

The frequency mapping matrix, J, of Equation (14) is now given as

$$\vec{j}_{\varpi 0+\Delta\omega} = J(\Delta\omega)\vec{j}_{\varpi 0} \approx \pm \frac{v_{y\omega 0+\Delta\omega}}{v_{y\varpi 0}} \tilde{T}(\varpi_0 + \Delta\omega)\tilde{T}^{-1}(\varpi_0)\vec{j}_{\omega 0} \tag{36}$$

Inspection of Equation (14) shows that the absolute value of the argument of the ratio of eigenvalues of J is equal to $\Delta\omega\Delta\tau$. Since multiplication by an arbitrary constant does not affect the ratio of eigenvalues, the ratio of the eigenvalues of the expression using the T estimates inside Equation (36) also yields the value of this ratio.

5.2.3 Poincaré sphere analysis

This analysis technique deduces the rotation angle, $\Delta\omega\Delta\tau$, directly.

Since the input SOPs, 0 and π/2 (sphere coordinates) are orthogonal, and the action of the input to output T matrix is that of a rotation, the associated output SOPs should be orthogonal on the sphere. A third orthogonal normalized Stokes vector representing what would be output from circular input SOP is calculated with the cross product operator. The measured output SOPs for both frequencies, ϖ_0 and $\varpi_0+\Delta\omega$, are adjusted to ensure orthogonality with the following

$$\vec{h} = \vec{H} \quad \vec{q} = \frac{\vec{H}\times\vec{Q}}{\left|\vec{H}\times\vec{Q}\right|}\times\vec{H} \quad \vec{v} = \frac{\vec{q}\times\vec{V}}{\left|\vec{q}\times\vec{V}\right|}\times\vec{q} \quad \vec{c} = \vec{h}\times\vec{q} \quad c' = \vec{q}\times\vec{v} \tag{37}$$

Also, calculate the associated difference vectors by subtracting the vector at ϖ_0 from the vector at $\varpi_0+\Delta\omega$ to obtain: $\Delta\vec{h}, \Delta\vec{q}, \Delta\vec{v}, \Delta\vec{c}, \Delta\vec{c}'$.

First, the situation for $\vec{h}, \vec{q}, \vec{c}$ is explained using Figures 7 and 8. Figure 7 shows a possible relationship of the PSP to the vectors obtained from Equation (37).

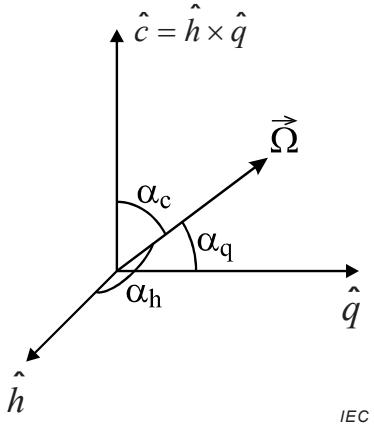

Figure 7 – Relationship of orthogonal output SOPs to the PDV

Figure 8 illustrates the rotation from one frequency to the next for an arbitrary output Stokes vector.

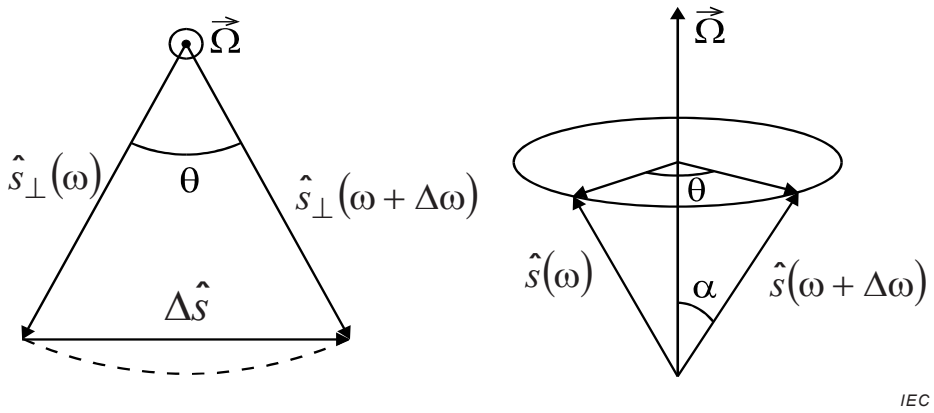

Figure 8 – Stokes vector rotation with frequency change

In Figure 8, $\hat{s}(\omega+\Delta\omega)$ is the component of $\vec{s}$ that is perpendicular to $\vec{\Omega}$, and θ is the rotation angle from which DGD, $\Delta\tau$, will be determined from the Stokes difference vector, $\Delta\vec{s} = \vec{s}(\varpi_0+\Delta\omega) - \vec{s}(\varpi_0)$. From geometrical considerations:

$$\left|\vec{s}_\perp\right| = \left|\sin\alpha\right| \quad \left|\Delta\vec{s}\right| = 2\left|\vec{s}_\perp\right|\left|\sin\frac{\theta}{2}\right| = 2\left|\sin\frac{\theta}{2}\right|\left|\sin\alpha\right| \tag{38}$$

Squaring both sides:

$$\Delta\vec{s}^{\,2} = \Delta\vec{s}\cdot\Delta\vec{s} = 4\sin^2\frac{\theta}{2}\sin^2\alpha \tag{39}$$

Collecting all the difference vectors lengths:

$$\Delta h^2 + \Delta q^2 + \Delta c^2 = 4\sin^2\frac{\theta}{2}\left(\sin^2\alpha_h + \sin^2\alpha_q + \sin^2\alpha_c\right)$$

$$= 4\sin^2\frac{\theta}{2}\left[3 - \left(\cos^2\alpha_h + \cos^2\alpha_q + \cos^2\alpha_c\right)\right]$$

$$= 8\sin^2\frac{\theta}{2} \tag{40}$$

The elimination of the sum of cosine terms is due to the cosine rule of three orthogonal vectors with respect to a common fourth vector. The sum of the cosine squared terms is equal to one.

From Equation (40), DGD is:

$$\Delta\tau = \frac{\theta}{\Delta\omega} = \frac{2}{\Delta\omega}\sin^{-1}\left[\left(\frac{\Delta\vec{h}^{\,2} + \Delta\vec{q}^{\,2} + \Delta\vec{c}^{\,2}}{8}\right)^{1/2}\right] \tag{41}$$

Using the alternative orthogonal Stokes vectors based on $\vec{V}$ yields a slightly improved estimate:

$$\Delta\tau = \frac{1}{\Delta\omega}\left\{\sin^{-1}\left[\left(\frac{\Delta\vec{h}^2 + \Delta\vec{q}^2 + \Delta\vec{c}^2}{8}\right)^{1/2}\right] + \sin^{-1}\left[\left(\frac{\Delta\vec{q}^2 + \Delta\vec{v}^2 + \Delta\vec{c}'^2}{8}\right)^{1/2}\right]\right\} \quad (42)$$

NOTE It is easily demonstrated that the PSA is also equivalent to the Mueller matrix method.

5.2.4 One ended measurements based on SPE [3]

IEC 61280-4-4 includes an informative measurement method based on measurements that can be done from one end of the transmission media. It is based on analysis of the output SOPs that are reflected from the far end and re-transmitted back toward the source where the reflected SOPs are measured with a polarimeter.

A directional coupler is inserted between the polarization controller and the transmission media. The transmission media is attached to the measurement equipment with a low loss angled connector. The reflected light goes through the directional coupler and into the polarimeter.

The far end of the transmission media shall reflect sufficient light so a flat end cut that is perpendicular to the fibre end might need to be prepared.

The reflected light is the sum of the Rayleigh scattering light and the light reflected from the far end. The following limitations must be evaluated:

- The far end reflected power dominates. This places a practical limit on the length measured.
- The Rayleigh scattering will normally be depolarized due to strong mode coupling. Degree of polarization of 90 % or more is preferred, but degree of polarization as low as 25 % can be measured – with reduced accuracy.

The basis of this technique is to write out the matrix, R_B, that maps input Stokes to output reflected Stokes as Equation (43).

$$R_B = MR^T MR \quad (43)$$

Where R is the forward transmission matrix and M is a diagonal matrix with elements (1,1,-1).

Like forward transmission, the DGD effect is deduced from the derivative expression:

$$\frac{ds_0}{d\omega} = \frac{dR_B}{d\omega} R_B^T s_0 = \Omega_B \times s_0 \quad (44)$$

It can be deduced that the reflected PDV is equal given as:

$$\Omega_{\boldsymbol{B}} = -2MR^T \begin{bmatrix} \Omega_1 \\ \Omega_2 \\ 0 \end{bmatrix} \quad (45)$$

Since the action of the rotations in Equation (45) have no effect on the length of the resulting vector, we can see that, in the context of strong mode coupling, the expected value of the length of this vector is related to the PMD RMS, hence linear average PMD, as Equation (46).

$$\left\langle \Delta\tau_B^2 \right\rangle = \frac{4 \cdot 2}{3} \left\langle \Delta\tau^2 \right\rangle = \pi \left\langle \Delta\tau \right\rangle^2 \tag{46}$$

Because the third element of Equation (45) is zero, the distribution of the length of φ_B is Rayleigh. This provides a relationship of the RMS to linear average given as:

$$\left\langle \Delta\tau_B^2 \right\rangle = \frac{4}{\pi} \left\langle \Delta\tau_B \right\rangle^2 \tag{47}$$

Combining Equations (46) and (47) yields Equation (48).

$$\left\langle \Delta\tau \right\rangle = \frac{2}{\pi} \left\langle \Delta\tau_B \right\rangle \tag{48}$$

5.3 Phase shift based measurement methods

5.3.1 General

There are two basic setups that are quite similar. These are illustrated in Figures 9 and 10.

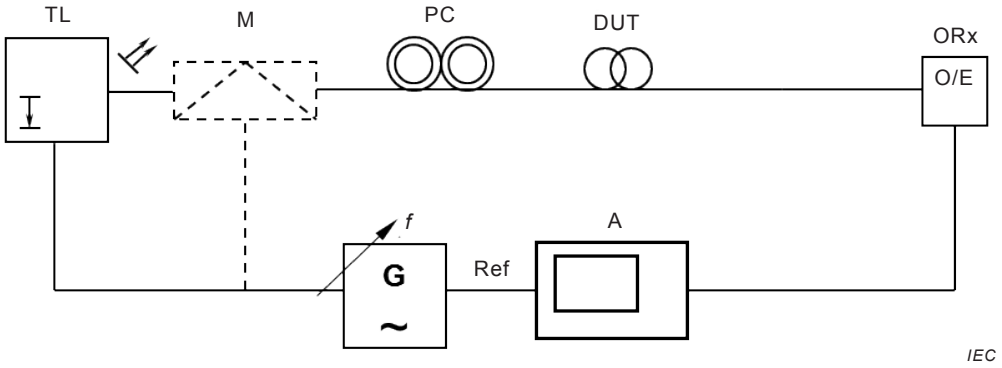

Key

TL tuneable laser
M modulator (optional)
PC polarization controller
ORx optical receiver
G HF oscillator tuneable in range 0,01 GHz to 10 GHz
A phase measurement analyzer

Figure 9 – Setup for modulation phase shift

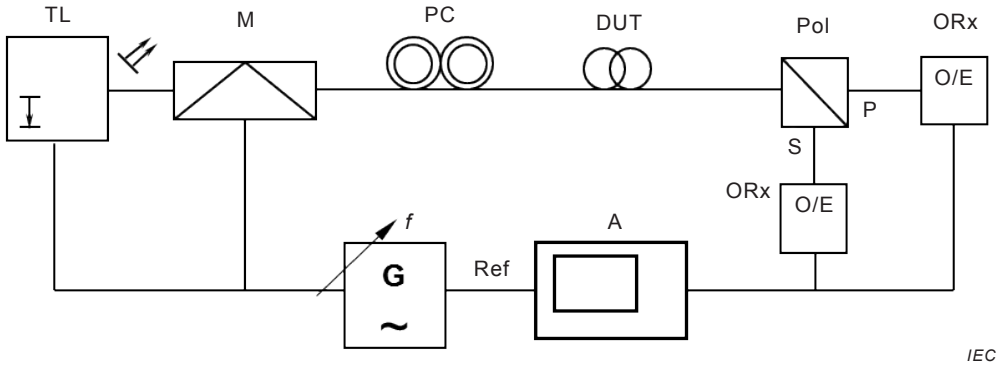

Key

TL tuneable laser

M modulator (optional)

PC polarization controller

Pol polarizer

ORx optical receiver

G HF oscillator tuneable in range 0,01 to 10 GHz

A amplitude / phase measurement analyzer

Figure 10 – Setup for polarization phase shift

For these methods, there is a scan of optical frequency yielding a DGD vs. frequency plot. For each optical frequency, there are a number of input SOPs that are launched. For each launch, the phase shift of a modulated optical signal is measured. For the MPS measurements, each optical frequency results in a DGD value. For the PPS measurement, each pair of adjacent optical frequencies produces a DGD value.

The main difference in the equipment is the polarization beam splitter used in the PPS method.

The individual test method standards have requirements on the modulation frequency that depend on the maximum DGD to be measured and the minimum resolution.

5.3.2 Modulation phase shift – Full search

The input SOP is varied over the full Poincaré sphere as pairs of orthogonal states. The phase difference for each orthogonal pair is calculated. The switching between orthogonal pairs may be modulated so phase difference measurements will not be affected by thermal drift.

The search is for the input pair that produces the maximum phase difference.

When the two orthogonal pairs are aligned with the fast and slow PSPs, the phase difference is maximal. A five degree difference between the true PSPs and the input SOPs will yield a DGD error of approximately 0,4 %. This forms a limit on the search density.

The DGD (ps) is obtained from the maximum phase difference, $\Delta\varphi_{max}$ (rad), and the modulation frequency, f (GHz) as

$$\Delta\tau = 1000\frac{\Delta\varphi_{\max}}{2\pi f} \tag{49}$$

Clearly, in an optical frequency scan, the PSPs of the last frequency can provide guidance on the approximate PSPs of the next optical frequency. This can be used to avoid doing an actual full SOP search for each optical frequency.

5.3.3 Modulation phase shift method – Mueller set analysis [4]

For each optical frequency, the input SOPs are cycled through the 4 Mueller states found in Table 2, where θ and μ are defined in Equations (6) and (10).

Table 2 – Mueller SOPs

Position	θ	μ	Description
A	0	0	Linear horizontal (H)
B	$\pi/4$	0	Linear 45 (Q)
C	$\pi/2$	0	Linear vertical (V)
D	$\pi/4$	$\pi/2$	Circular (C)

The phase of each position is measured and labelled φ_A, φ_B, φ_C, and φ_D.

The average of phases A and C is calculated and then subtracted from the phases for positions A, B, and D, which are labelled as δ_A, δ_B, and δ_D. Finally, these are combined in Equation (50).

$$\delta = 2\tan^{-1}\left\{\left[\tan^2\delta_A + \tan^2\delta_B + \tan^2\delta_D\right]^{1/2}\right\} \tag{50}$$

This is converted to DGD (ps) using the modulation frequency, f (GHz), and Equation (51).

$$\Delta\tau = 1000\frac{\delta}{2\pi f} \tag{51}$$

The next paragraphs form an attempt to explain Equation (50).

An arbitrary output Jones vector can be written as a linear combination of the two orthogonal PSP Jones vectors. The two components have phase shifts of $\Phi+\delta$ and $\Phi-\delta$. Φ is the polarization independent due to both the systems mean group delay and electronic delays. The polarization dependent part is δ. The power of the two components can be related to the angle, α (Poincaré sphere angle), between the PSP and output SOP on the Poincaré as $\cos^2(\alpha/2)$ and $\sin^2(\alpha/2)$.

The phase detector yields the phase resulting from the sum of the two components, which can be shown to follow Equation (52).

$$\phi = \tan^{-1}\left(\cos\alpha\tan\frac{\delta}{2}\right) + \Phi \tag{52}$$

Figure 11 shows an output SOP, S, and its relationship to the PSP.

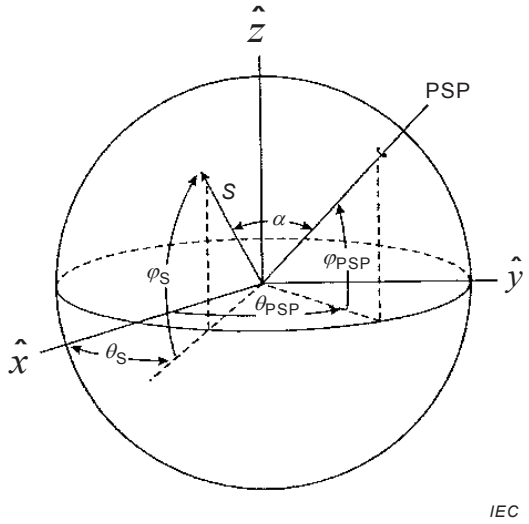

Figure 11 – Output SOP relation to the PSP

From Figure 11, Equation (53) can be deduced.

$$\alpha = \cos^{-1}[\cos\varphi_{PSP}\cos(\theta_{PSP} - \theta_S)] \tag{53}$$

Thus far, the discussion has been with respect to an arbitrary output SOP, which, in general, has an unknown relationship to an input SOP. In the case of the Mueller input set, which forms an orthogonal framework, we can conclude that the output SOPs will also form an orthogonal basis because the action of the T matrix is a rotation. This means that there is a rotated reference frame wherein the output SOPs form the Mueller set. The following results from the application of Equations (52) and (53) in that rotated reference frame.

For the linear SOPs, the measured phases follow:

$$\phi_A = \tan^{-1}\left(\cos\varphi_{PSP}\cos\theta_{PSP}\tan\frac{\delta}{2}\right) + \Phi \tag{54}$$

$$\phi_B = \tan^{-1}\left(\cos\varphi_{PSP}\sin\theta_{PSP}\tan\frac{\delta}{2}\right) + \Phi \tag{55}$$

$$\phi_C = -\tan^{-1}\left(\cos\varphi_{PSP}\cos\theta_{PSP}\tan\frac{\delta}{2}\right) + \Phi \tag{56}$$

Equation (56) is derived from the fact that SOP C is orthogonal to SOP A.

Since SOP D is not on the equator, but for this special case, $\alpha = \pi/2 - \varphi_{PSP,}$ so:

$$\phi_D = \tan^{-1}\left(\sin\varphi_{PSP}\tan\frac{\delta}{2}\right) + \Phi \tag{57}$$

It is clear that when the average of phase A and phase C are subtracted from the A, B, and D phase measurement, the $\tan^{-1}$ terms remain as δ_A, δ_B, and δ_D. The sum of $\tan^2\delta_A$ and $\tan^2\delta_B$ yields $\cos^2{}_{\varphi PSP}\tan^2\delta/2$. Addition of $\tan^2\delta_D$ yields $\tan^2\delta/2$. Equation (50) follows easily.

5.3.4 Polarization phase shift measurement method[5]

5.3.4.1 PPD measurements and calculations

A scan of optical frequencies is made. Adjacent pairs of frequencies produce DGD values. For each frequency, the input polarizer is set to linear 0 and $\pi/2$ SOPs. The phase and power for the P and S states are measured after the polarization splitter. The results for each frequency can be represented by the following matrix:

$$U = \begin{bmatrix} P_{11}\exp(-i\Phi_{11}) & P_{12}\exp(-i\Phi_{12}) \\ P_{21}\exp(-i\Phi_{21}) & P_{22}\exp(-i\Phi_{22}) \end{bmatrix} \tag{58}$$

Input SOPs are columns and P/S states are rows.

Index the frequencies with k and for k = 1 to n-1.

Calculate the phase derivatives for the data defined in Equation (56).

For I = 1,2, j = 1,2:

$$\Phi'_{ijk} = \frac{\Phi_{ij(k+1)} - \Phi_{ijk}}{\Delta\omega} \tag{59}$$

Then calculate the following:

$$\cos 2\theta_k = \frac{P_{11k} - P_{21k}}{P_{11k} + P_{21k}} \tag{60}$$

$$\theta_k = \frac{1}{2}\cos^{-1}(\cos 2\theta_k) \tag{61}$$

$$\theta'_k = \frac{\theta_{k+1} - \theta_k}{\Delta\omega} \tag{62}$$

$$\phi'_k = (\Phi'_{11k} - \Phi'_{22k} - \Phi'_{21k} + \Phi'_{12k})/4 \tag{63}$$

$$\psi'_k = (\Phi'_{11k} - \Phi'_{22k} + \Phi'_{21k} - \Phi'_{12k})/4 \tag{64}$$

$$\Delta\tau_k = 2\left[\psi'^2_k + \varphi'^2_k + \theta'^2_k + 2\psi'_k\phi'_k\cos 2\theta_k\right]^{1/2} \tag{65}$$

Finally, calculate the PMD value using either the linear average or RMS of the $\Delta\tau_k$ values.

5.3.4.2 PPD Theory

The input to output Jones matrix that maps an arbitrary input Jones vector to the output vector is T. For this measurement method, it is formulated somewhat differently than the formulation used to see the rotational aspects (as in Clause 4). In particular, the θ parameter here is not the same as the parameter used in defining the rotation vector.

$$T = \begin{bmatrix} \cos\theta \exp(-i\psi_1) & -\sin\theta \exp(i\psi_2) \\ \sin\vartheta \exp(-i\psi_2) & \cos\theta \exp(i\psi_1) \end{bmatrix} = \begin{bmatrix} \cos\theta \exp[-i(\psi+\phi)] & -\sin\theta \exp[i(\psi-\phi)] \\ \sin\theta \exp[-i(\psi-\phi)] & \cos\theta \exp[i(\psi+\phi)] \end{bmatrix} \quad (66)$$

where all parameters are functions of frequency and:

$$\begin{bmatrix} \phi \\ \psi \end{bmatrix} = \frac{1}{2} \begin{bmatrix} 1 & -1 \\ 1 & 1 \end{bmatrix} \begin{bmatrix} \psi_1 \\ \psi_2 \end{bmatrix} \quad (67)$$

The relationship to DGD is through the D matrix, the eigenvalues of which are equal to $\pm i\Delta\tau/2$, as shown in Equation (19).

$$D = \frac{dT}{d\varpi} T^{-1} = \begin{bmatrix} -i(\psi' \cos 2\theta + \phi') & -(\theta' + i\psi' \sin 2\theta)\exp(-i2\phi) \\ (\theta' - i\psi' \sin 2\theta)\exp(i2\phi) & i(\psi' \cos 2\theta + \phi') \end{bmatrix} \quad (68)$$

The rightmost formulation in Equation (66) enables this clean expression of D. The variables with a "prime", e.g., ψ', are frequency derivatives.

The eigenvalues of D are obtained by finding λ such that

$$\det(D - \lambda I) = 0 \quad (69)$$

where

det is the determinant operator;

I is the identity matrix.

Equation (69) evaluates to:

$$\lambda^2 + (\psi' \cos 2\theta + \phi')^2 + \theta' + \psi' \sin^2\theta = \lambda^2 + \psi'^2 + \varphi'^2 + \theta'^2 + 2\psi'\phi' \cos 2\theta = 0 \quad (70)$$

The DGD is therefore given as:

$$\Delta\tau = 2\left[\psi'^2 + \varphi'^2 + \theta'^2 + 2\psi'\phi' \cos 2\theta\right]^{1/2} \quad (71)$$

The first two derivatives in Equation (70) are obtained from the following, which link Equation (58), the measurements, to the first formulation of Equation (66).

$$\psi_1' \approx \Phi_{11}' \approx -\Phi_{22}' \text{ so } \psi_1' = \frac{\Phi_{11}' - \Omega_{22}'}{2} \quad (72)$$

$$\psi_2' \approx \Phi_{21}' \approx -\Phi_{12}' \text{ so } \psi_2' = \frac{\Phi_{21}' - \Omega_{12}'}{2} \quad (73)$$

Application of Equation (67) yields:

$$\begin{bmatrix} \phi' \\ \psi' \end{bmatrix} = \frac{1}{4} \begin{bmatrix} \Phi_{11}' - \Phi_{22}' - \Phi_{21}' + \Phi_{12}' \\ \Phi_{11}' - \Phi_{22}' + \Phi_{21}' - \Phi_{12}' \end{bmatrix} \quad (74)$$

Inspection of Equations (58) and (66) shows that P_{11} and P_{21} are proportional to $\cos^2\theta$ and $\sin^2\theta$. As a consequence, we have:

$$\cos 2\theta = \frac{P_{11} - P_{21}}{P_{11} + P_{21}} \tag{75}$$

This must be calculated for each frequency. The arccos of these values, divided by two, yields θ values for each frequency, hence the frequency derivatives $\theta'_k = (\theta_{k+1} - \theta_k)/\Delta\omega$.

The arccos function returns values between 0 and π. The real 2θ function might go from values in this range to values in excess of π. Since there is no information on $\sin 2\theta$, this situation cannot be determined from the data, only guessed. There could be a requirement to make a guess based on continuity, for example, but in 5.3.4.1, there is no such requirement.

Maintaining an assumption that 2θ is between 0 and π has no effect on the accuracy of the $\cos 2\theta$ term. It could affect the derivative for the frequency that just crosses 0 or π, but since the square of the derivative is used in the calculation, this change in derivative is expected to have a small effect on the overall PMD.

In [5], an additional term for group delay is added to the T matrix. It is a multiplication by $\exp(-i\Phi)$. It is stated that the group delay time independent of polarization is obtained as $\tau_g = (\Phi'_{11} + \Phi'_{22})/2$.

5.4 Interferometric measurement methods

5.4.1 General

A generic setup for interferometric method is shown in Figure 12.

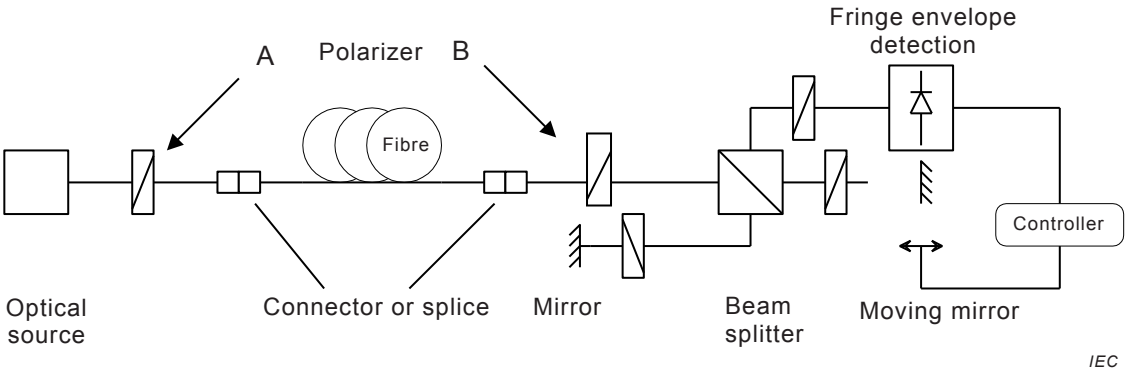

Figure 12 – Interferometric measurement setup

Figure 12 is most representative of the TINTY method. For GINTY, polarization scramblers are placed after polarizer A and before polarizer B. In addition, for GINTY, there is a requirement to make measurements with polarizer B at: a) an arbitrary setting and b) a setting orthogonal to the first setting. Depending on the equipment, this can be done in various ways.

NOTE 1 For GINTY, the polarization scrambling function could be done with the polarizers, depending on the polarizer design.

The optical source is an unpolarised broadband light source with constant autocorrelation function and no deterministic modulation. For TINTY, a spectrum that is approximately Gaussian with no ripples is needed.

The interferogram will first be explained in terms of the setup with polarizer B removed.

If the source were monochromatic with angular optical frequency of ω_0, the field at the detector would be the sum of the fields displaced by t_1 and t_2, the distances of the two arms of the interferometer.

$$E(t_1 - t_2) = \frac{1}{2} E_0 \{\exp[-i\omega_0(t - t_1)] + \exp[-i\omega_0(t - t_2)]\}$$

$$= \frac{1}{2} E_0 \exp[-\omega_0(t - t_1)]\{1 + \exp[-i\omega_0(t_1 - t_2)]\} \quad (76)$$

The power is given as:

$$E^*(t_1 - t_2)E(t_1 - t_2) = \frac{1}{4} E_0^2 \{2 + \exp[-i\omega_0(t_1 - t_2)] + \exp[i\omega_0(t_1 - t_2)]\}$$

$$= \frac{1}{2} E_0^2 \{1 + \cos[\omega_0(t_1 - t_2)]\}$$

$$= \frac{1}{2} E_0^2 (1 + \cos(\omega_0 \tau)) \quad (77)$$

For a polychromatic source with spectrum, $S_0(\omega)$, the power detected by the interferometer is given as Equation (78).

$$I_0(\tau) = \frac{1}{2} \int S_0(\omega) d\omega + \frac{1}{2} \int S_0(\omega) \cos(\tau\omega) d\omega = P_{Const} + \tilde{P}_0(\tau) \quad (78)$$

The second part of Equation (78) is closely related to the autocorrelation function of the source, $R(\tau)$ as:

$$R(\tau) = \int S_0(\omega) \exp[i\tau\omega] d\omega = \left\langle E(t) E^*(t - \tau) \right\rangle \quad (79)$$

The constant term in Equation (78) shall be subtracted before further calculations and can easily be done because the two terms are equal when τ = 0. This subtraction will be assumed to be done for the rest of the interferometric method descriptions.

The reason for the 0 subscript in Equations (78) and (79) is that this is the spectrum before polarizer B. The power after polarizer B (an analyser) is designated as $S(\omega)$ and is given as Equation (80).

$$S(\omega) = \frac{1}{2} S_0(\omega)(1 + \vec{s}(\omega) \cdot \vec{s}_a) = \frac{1}{2} S_0(\omega)(1 + x(\omega)) = \frac{1}{2}(S_0(\omega) + S_x(\omega)) \quad (80)$$

There are some different notations for the different parts of the derivation that are found in Equation (80). The main part is shown in the first term, where the output Stokes vector, $\vec{s}(\omega)$, appears in a dot product with the Stokes vector, $\vec{s}_a$, which is the orientation of polarizer B. This dot product is called $x(\omega)$ in the second expression of Equation (79). PMD is related to the variance of the output SOP with angular optical frequency. The characterization of the variance of the dot product, $x(\omega)$, through the interferogram, is the basis of the interferometric method.

The non-constant part of the interferogram after polarizer B is given as Equation (81).

$$\tilde{P}(\tau) = \frac{1}{2}\int S_0(1 + x(\omega))\cos(\omega\tau)d\omega \tag{81}$$

Figure 13 shows some of the relationships defined above graphically.

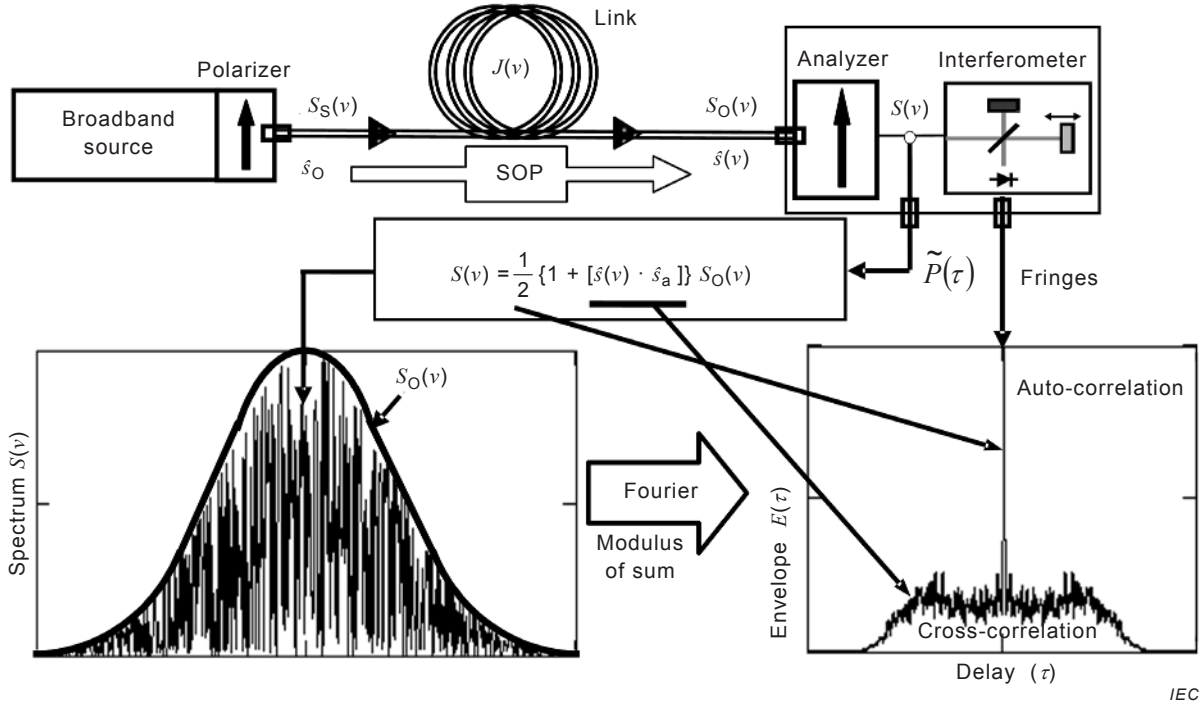

Figure 13 – Interferogram relationships

The interferogram part of Figure 13 is actually the absolute value of the result of Equation (81). It shows a central peak, which is labelled "auto-correlation". This is the result of the “1” part of (1+$x(\omega)$) in Equation (81). Its width decreases as the spectrum broadens. The other part, due to $x(\omega)$, is called the "cross correlation". Its width increases as PMD increases.

NOTE 2 Polarizer B is often called an *analyzer*.

5.4.2 Generalized interferometric method [6]

5.4.2.1 Cosine transform pair characteristics

This subclause shows some relationships of cosine transform pairs. 5.4.1 showed that the interferogram and spectra are related by way of cosine transforms. Two results from this clause, Equations (87) and (88), will be used in 5.4.2.2 to follow.

Define F and f as a cosine pair.

$$f(\tau) = \sqrt{\frac{2}{\pi}}\int_0^\infty F(\omega)\cos(\omega\tau)d\omega \tag{82}$$

$$F(\omega) = \sqrt{\frac{2}{\pi}} \int_0^\infty f(\tau)\cos(\omega\tau)d\tau \tag{83}$$

$$F^2(\omega) = \frac{2}{\pi} \int_0^\infty \int_0^\infty f(\tau)f(\tau')\cos(\omega\tau)\cos(\omega\tau')d\tau d\tau' \tag{84}$$

$$\int_0^\infty F^2(\omega)d\omega = \frac{2}{\pi} \int_0^\infty \int_0^\infty f(t)f(\tau') \int_0^\infty \cos(\omega\tau)\cos(\omega\tau')d\omega d\tau d\tau' \tag{85}$$

The integral with respect to frequency is a delta function such that:

$$\int_0^\infty \int_0^\infty f(\tau)f(\tau')\cos(\omega\tau)\cos(\omega\tau')d\omega d\tau' = f^2(t) \tag{86}$$

Substituting into Equation (85):

$$\int_0^\infty F^2(\omega)d\omega = 2\int_0^\infty f^2(\tau)d\tau = \int_{-\infty}^\infty f^2(\tau)d\tau \tag{87}$$

The rightmost expression of Equation (87) is allowed because the ideal interferogram is even about zero.

Taking a similar path results in Equation (88) for the derivative of F with respect to frequency.

$$\int_0^\infty \left[\frac{dF(\omega)}{d\omega}\right]^2 d\omega = \int_{-\infty}^\infty \tau^2 f^2(\tau)d\tau \tag{88}$$

5.4.2.2 Separation of autocorrelation from cross correlation functions

Following the notation of IEC 61280-4-4, the two non-constant interferogram terms for the initial and orthogonal polarizer B settings are designated as $\tilde{P}_x(\tau)$ and $\tilde{P}_y(\tau)$. Continuing the notation of IEC 61280-4-4, Equations (89) and (90) yield the autocorrelation and cross correlation functions, respectively, because the $x(\omega)$ function in Equation (80) for the orthogonal setting is the negative of the initial setting.

$$E_0(\tau) = \tilde{P}_x(\tau) + \tilde{P}_y(\tau) \quad E_x(\tau) = \tilde{P}_x(\tau) - P_y(\tau) \tag{89}$$

Further consideration of Equation (79) shows that E_0 and E_x are cosine transform pairs with S_0 and S_x, respectively.

Polarization scrambling is recommended. There are various ways to do this, including Mueller set sampling for both the launch and receive ends. Mueller set sampling includes all permutations of states A, B, and D from Table 2 for both input and output.

Polarization scrambling results in the mean square envelopes for both the autocorrelation and cross correlation functions, which are given in Equation (90).

$$\overline{E}_0^2(\tau) = \frac{1}{N}\sum_i E_{0i}^2(\tau) \quad \overline{E}_x^2(\tau) = \frac{1}{N}\sum_i E_{xi}^2(\tau) \tag{90}$$

From the relationships of 5.4.2.1:

$$\int_{-\infty}^{\infty} \overline{E}_0^2(\tau)d\tau = \int_0^{\infty} S_0^2(\omega)d\omega \quad \int_{-\infty}^{\infty} \tau^2 \overline{E}_0^2(\tau)d\tau = \int_0^{\infty} \left[\frac{dS_0(\omega)}{d\omega}\right]^2 d\omega \tag{91}$$

$$\int_{-\infty}^{\infty} \overline{E}_x^2(\tau)d\tau = \int_0^{\infty} \left\langle S_x^2(\omega)\right\rangle d\omega \quad \int_{-\infty}^{\infty} \tau^2 \overline{E}_x^2(\tau)d\tau = \int_0^{\infty} \left\langle \left[\frac{dS_x(\omega)}{d\omega}\right]^2 \right\rangle d\omega \tag{92}$$

The expected value operators in these equations are with respect to scrambler states.

Equations (91) and (92) show the calculation of the RMS widths and their relationship to the spectra.

$$\sigma_0^2 = \frac{\int_{-\infty}^{\infty} \tau^2 \overline{E}_0^2(\tau)d\tau}{\int_{-\infty}^{\infty} \overline{E}_0^2(\tau)d\tau} = \frac{\int_0^{\infty} \left[\frac{dS_0(\omega)}{d\omega}\right]^2 d\omega}{\int_0^{\infty} S_0^2(\omega)d\omega} \tag{93}$$

$$\sigma_x^2 = \frac{\int_{-\infty}^{\infty} \tau^2 \overline{E}_x^2(\tau)d\tau}{\int_{-\infty}^{\infty} \overline{E}_x^2(\tau)d\tau} = \frac{\int_0^{\infty} \left\langle \left[\frac{dS_x(\omega)}{d\omega}\right]^2 \right\rangle d\omega}{\int_0^{\infty} \left\langle S_x^2(\omega)\right\rangle d\omega} \tag{94}$$

The following Figure 14 shows mean square envelope examples for $\overline{E}_x^2$ and $\overline{E}_0^2$.

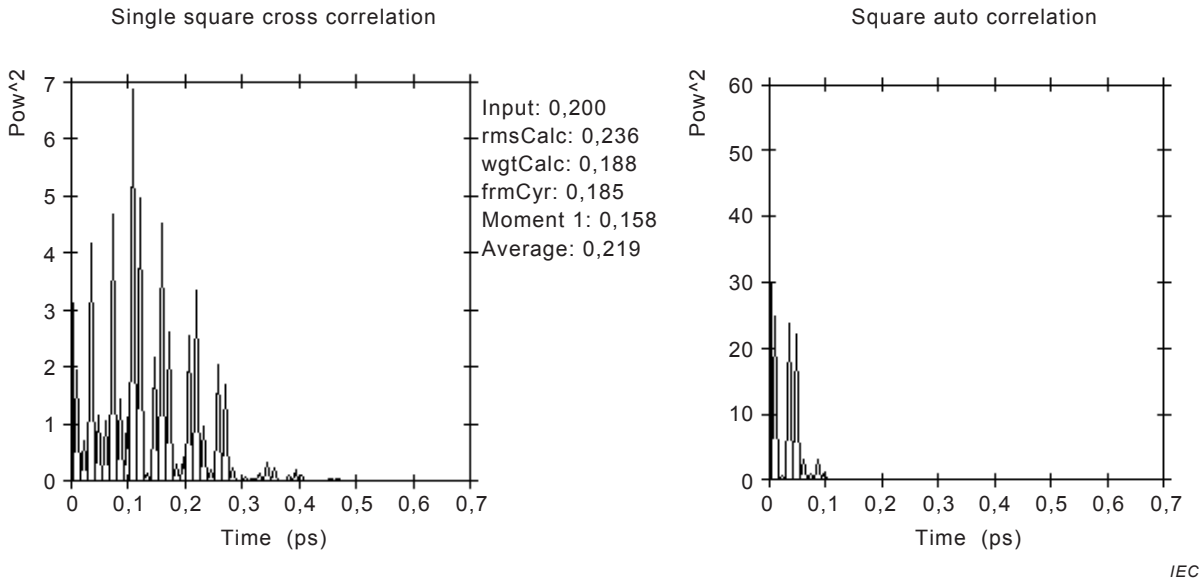

Figure 14 – Mean square envelopes

5.4.2.3 Relationship to PMD

This subclause will connect the results from 5.4.2.1 and 5.4.2.2 to the RMS PMD. The expected value operator is with respect to scrambler state.

The definition of the cross correlation spectrum, S_x, leads to Equation (95).

$$\left\langle \left[\frac{dS_x(\omega)}{d\omega} \right]^2 \right\rangle = \left\langle \left(\frac{dx(\omega)}{d\omega} \right)^2 \right\rangle S_0^2(\omega) + 2\left\langle x(\omega)\frac{dx(\omega)}{d\omega} \right\rangle S_0(\omega)\frac{dS_0(\omega)}{d\omega} + \left\langle x^2(\omega) \right\rangle \left(\frac{dS_0(\omega)}{d\omega} \right)^2 \quad (95)$$

The following properties assume that the statistics of the input Stokes vector, which are assumed to be random, are the same as the statistics of the output Stokes vector.

- The probability distribution functions of the individual Stokes vector elements si, are uniformly distributed as ½.
- They are uncorrelated: $\langle s_i s_j \rangle = 0, i \neq j$
- Expected value of the square: $\langle s_i^2 \rangle = 1/3$
- Uncorrelated with polarizer B: $\langle \vec{s} \cdot \vec{s}_a \rangle = 0$

Implications of these relationships follow:

$$\langle x^2(\omega) \rangle = 1/3 \Rightarrow \langle S_x^2(\omega) \rangle = \frac{1}{3} S_0^2(\omega) \quad (96)$$

$$\left\langle \frac{dx(\omega)}{d\omega} x(\omega) \right\rangle = 0 \quad (97)$$

$$\left\langle \left[\frac{dx(\omega)}{d\omega} \right]^2 \right\rangle = \frac{1}{3} \left\langle \frac{d\vec{s}}{d\omega} \cdot \frac{d\vec{s}}{d\omega} \right\rangle = \frac{1}{3} \left\langle \left| \frac{d\vec{s}}{d\omega} \right|^2 \right\rangle \tag{98}$$

Equation (95) can now be written as Equation (99).

$$\left\langle \left[\frac{dS_x(\omega)}{d\omega} \right]^2 \right\rangle = \frac{1}{3} S_0^2(\omega) \left\langle \left| \frac{d\vec{s}(\omega)}{d\omega} \right|^2 \right\rangle + \frac{1}{3} \left[\frac{dS_0(\omega)}{d\omega} \right]^2 \tag{99}$$

From Equation (18), where everything is a function of frequency:

$$\frac{d\vec{s}(\omega)}{d\omega} = \vec{\Omega} \times \vec{s} = \Delta\tau \left(\vec{p} \times \vec{s} \right) = \left(\Delta\tau \sin\theta \right) \vec{u} \tag{100}$$

where

θ is the random angle between $\vec{s}$ and $\vec{p}$;

$\vec{u}$ is the unit vector perpendicular to them.

Equation (98) leads to Equation (101) because of the random relationship of the output Stokes vector to the PSP.

$$\left\langle \left| \frac{d\vec{s}(\omega)}{d\omega} \right|^2 \right\rangle = \Delta\tau^2 \left\langle \sin^2(\theta) \right\rangle = \frac{2}{3} \Delta\tau^2 \tag{101}$$

Integrating Equation (99) and dividing by $\int_0^\infty \left\langle S_x^2(\omega) \right\rangle dw = \frac{1}{3} \int_0^\infty S_0^2(\omega) d\omega$ yields Equation (102).

$$\frac{\int_0^\infty \left\langle \left[\frac{dS_x(\omega)}{d\omega} \right]^2 \right\rangle d\omega}{\int_0^\infty \left\langle S_x^2(\omega) \right\rangle d\omega} = \frac{2}{3} \frac{\int_0^\infty \Delta\tau^2 S_0^2(\omega) d\omega}{\int_0^\infty S_0^2(\omega) d\omega} + \frac{\int_0^\infty \left[\frac{dS_0(\omega)}{d\omega} \right]^2 d\omega}{\int_0^\infty S_0^2(\omega) d\omega} \tag{102}$$

This leads to the PMD formula that is found in IEC 61280-4-4.

$$\left[\frac{3}{2} \left(\sigma_x^2 - \sigma_0^2 \right) \right]^{1/2} = PMD_{RMS} = \left[\frac{\int_0^\infty \Delta\tau^2 S_0^2(\omega) d\omega}{\int_0^\infty S_0^2(\omega) d\omega} \right]^{1/2} \tag{103}$$

The PMD_{RMS} value that is reported is a power-squared weighted RMS value.

5.4.2.4 Mueller matrix scrambling

When the 9 I/O SOPs that represent all permutations of the three Mueller input states with the three output states are used, it can be confirmed that the relationships leading to the result of 5.4.2.4 are produced.

The output SOPs, $\vec{s}_a$, form the columns of the identity matrix. The input SOPs are also the columns of the identity matrix, but the output states are the columns of a rotation matrix. A random rotation matrix can be built with a random rotation vector and angle using Equation (12).

A first aspect to be confirmed is $\langle s_i s_j \rangle = 0, i \neq j$. This is confirmed by forming all such products for the rotation matrix and summing. The sum is invariably zero. It is clearly true for the identity matrix.

A second aspect to be confirmed is $\left(s_i^2\right) = 1/3$. This is confirmed for the rotation matrix by averaging the squares of all elements. It is also clearly valid for the identity matrix. Considering that the $9\times$ values are the 9 elements of the rotation matrix, the property, $\langle x^2 \rangle = 1/3$ is also confirmed.

A property that is not confirmed is $\langle \vec{s} \cdot \vec{s}_a \rangle = 0$. The sum of the rotation matrix elements is not zero. The consequence is that the expected value of certain expressions cannot be determined independently for the two vectors. One such expression is Equation (97). This evaluates to Equation (104) for the Mueller output set.

$$\frac{dx(\omega)}{d\omega} x(\omega) = \frac{ds_1}{d\omega} s_1 s_{a1}^2 + \frac{ds_2}{d\omega} s_2 s_{a2}^2 + \frac{ds_3}{d\omega} s_3 s_{a3}^2 \tag{104}$$

When Equation (104) is averaged over the three Mueller output states, where if one element of $\vec{s}_a$ is one, the other two elements are zero, one obtains the dot product of the derivative of a normalized Stokes vector with itself. This has a value of zero, so Equation (97) is confirmed.

Another relationship that could need independence of the two vectors is Equation (98). This expands to Equation (105).

$$\left[\frac{dx(\omega)}{d\omega}\right]^2 = \left(\frac{ds_1}{d\omega}\right)^2 s_{a1}^2 + \left(\frac{ds_2}{d\omega}\right)^2 s_{a2}^2 + \left(\frac{ds_3}{d\omega}\right)^2 s_{a3}^2 \tag{105}$$

Averaging over the Mueller three output states yields an equation like Equation (103) for one input vector. Averaging across three input vectors yields the full Equation (98).

As a consequence of the above, all the relationships leading to Equation (102) are satisfied by using the permutations of the three input and output Mueller states.

5.4.3 Traditional interferometric measurement method

This method suffers from the following deficiencies:

- no separation of the cross correlation function from the auto correlation function;
- it works with the absolute values of the $\tilde{P}(\tau)$ functions rather than the squares;
- the spectrum must be close to Gaussian and without ripples;

- strong mode coupling must be assumed, like in the fixed analyser method.

5.5 Fixed analyser

5.5.1 General

A typical equipment setup is shown in Figure 15.

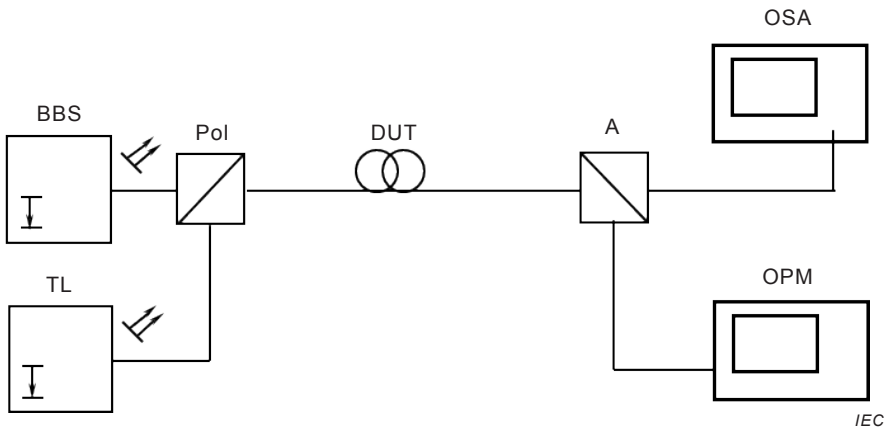

Key

BBS	broadband source
TL	tuneable laser
Pol	polarizer (1SOP)
A	analyzer (0° or 90°)
OSA	optical spectrum analyzer
OPM	optical power meter

Figure 15 – Fixed analyser setup

The source may either be a tuneable laser or a broadband source. Depending on which, either an optical power meter or a spectrum analyser is used to measure output power vs. optical frequency. As with the DGD-based methods, the standards provide guidance on the frequency increment and extent, depending on the expected maximum PMD.

If a broadband source is used, it should follow the requirements used for the interferometric method.

The analyser, which is really a polarizer, shown in Figure 15 is indicated with a capability of being switched to either of a pair of orthogonal orientations. Although this is not formally required by the International Standards, the findings of the GINTY show that the sum and difference of these power functions allow separation of the autocorrelation and cross correlation functions and the separation of S_0 and S_x.

Addition of polarization scramblers after the polarizer and before the analyser would allow collection of data across all permutations of the Mueller states for input and output, yielding an improvement in results consistent with GINTY results.

What is measured is either $P_A(v)$ and $P_{tot}(v)$ or $P_A(v)$ and $P_B(v)$

where

$P_A(v)$ is the power spectrum measured with the analyser in place

$P_{tot}(v)$ is the power with the analyser taken away

$P_B(v)$ is the power with the analyser set orthogonal to the initial setting

Given the results of GINTY, the difference between P_A and P_B leads to the cross-correlation function because the analyser/polarizer for setting B is orthogonal to setting A. In some International Standards, such as IEC 60793-1-48, it is mentioned that a polarimeter could be substituted for the analyser/detector combination. In this case, the three Stokes elements are each the normalized difference in powers between two orthogonal states. Furthermore, the three elements are a complete Mueller output set. The three should be combined in squared power for the cosine Fourier transform technique or for the spectral differentiation technique. Combining three Mueller input SOPs with the paired Stokes output vectors forms a complete Mueller input/output set.

While the International Standards allow equal increment in wavelength, this Technical Report will define results in terms of optical frequency, either angular, ω, or just 1/t units, v, e.g., GHz. It is better to use equal increments of frequency so the transform methods can be used.

The first three items on the list of analysis methods are in the current standards and appear in the order that they were discovered. The last is not currently in any International Standard, but is derived from the mathematics of GINTY.

- extrema counting;
- Fourier transform;
- cosine Fourier transform;
- spectral differentiation.

5.5.2 Extrema counting

The ratio function, $R(v)$, is calculated as either

$$R(v) = \frac{P_A(v)}{P_{tot}(v)} \text{ or } R(v) = \frac{P_A(v)}{P_A(v) + P_B(v)} \tag{106}$$

This produces a result such as what is shown in Figure 16.

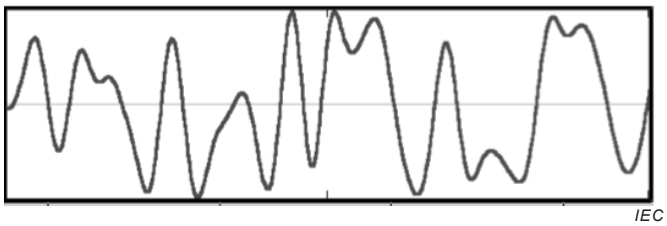

Figure 16 – Fixed analyser ratio

This measurement method and analysis technique was the first proposed in standardization activities. The variation seen in Figure 16 is due to the variance in the output SOP with frequency. The formula for obtaining the linear average PMD value is Equation (107).

$$\langle \Delta\tau \rangle = k \frac{E}{2(v_2 - v_1)} \tag{107}$$

Where

E is the number of extrema, either maxima or minima;

v_1 and v_2 define the range of frequencies that were measured.

The parameter k is usually given as 1 for the case of negligible mode coupling and 0,824 for random mode coupling, but it can only be considered as an approximation for the case of strong mode coupling or intermediate mode coupling.

Figure 16 shows a case of strong random mode coupling. Negligible mode coupling would show a simple sinusoidal function.

Equation (107) was the result of simulations combined with experimental observations and comparisons of birefringence measurements and deployed long lengths.

The extrema counting technique was the first proposed in standards at a time when PMD was not generally very well understood or specified, and the first priority was sorting out very bad cables from moderate to good cables. It served its purpose but at this time, Equation (105) is best used to illustrate how the variance increases as PMD increases, which provides guidance on what frequency increment should be used. Also, Gisin [2] used it to estimate PMD measurement repeatability as a function of frequency extent.

A frequency extent sufficient to produce 10 extrema is recommended.

5.5.3 Fourier transform

This technique is also based on the ratio functions of Equation (106). The Fourier transform of this function converts data from the frequency domain to the time domain in a manner that is similar to the interferometer. As we see in the GINTY, the result of doing an FFT on the ratio is FFT(1/2(1+$x(\omega)$)). The ½ part of this creates a $\sin(x)/x$ type of response so the general recommendation is to use a windowing function that goes to zero smoothly at the frequency extremes.

Equal increments of frequency are required. The International Standards allow fitting and interpolation to obtain equal increments in frequency from data that are based on equal wavelength increments. The FFT requires an input array with the number of elements equal to a power of 2. When the measurements do not occupy the whole array, zero-padding or filling the part not occupied with zeros should be done.

For a broadband source, a good windowing function would be the spectrum before the analyser, P_{tot}, or $P_{A+PB,}$ which are S_0 from the GINTY discussion. For a tuneable laser, something that looks similar to a Gaussian source should be used. When this is done, the FFT produces something close to an interferogram. The FFT is the sum of the autocorrelation function and the cross correlation function – but it is a complex result. While not actually stated, the $P(\tau)$ functions (results from the FFT) in the standards are the result of multiplying the complex number Fourier transform value for a given time with its complex conjugate. In this way the plot of $P(\tau)$ is similar to the squared interferogram envelope.

In the International Standards, it is stated that care shall be taken to remove, or avoid using, the part of the transform near 0. This is the part of the transform that is dominated by the autocorrelation function. When P_A and P_B are measured, a better way to remove the autocorrelation function would be to do the FFT on $P_A \_ P_B$. This is prescribed in the cosine Fourier transform technique.

Figures 17 and 18 show a post analyser spectrum and its Fourier transform power function. It seems clear that this Fourier transform was done on the spectrum directly.

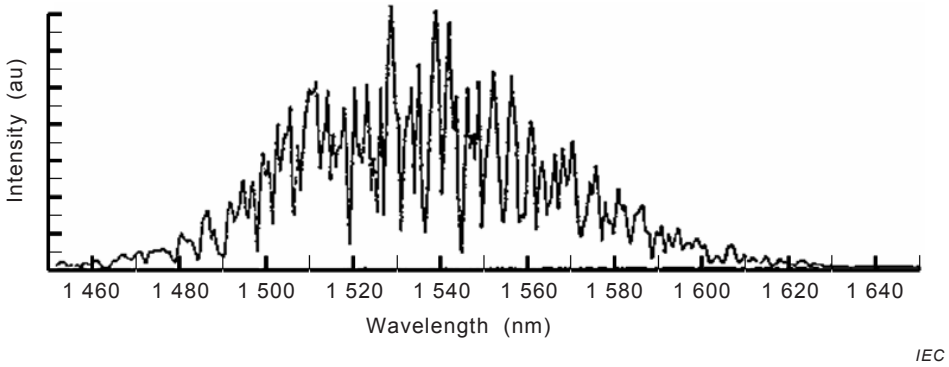

Figure 17 – Power spectrum

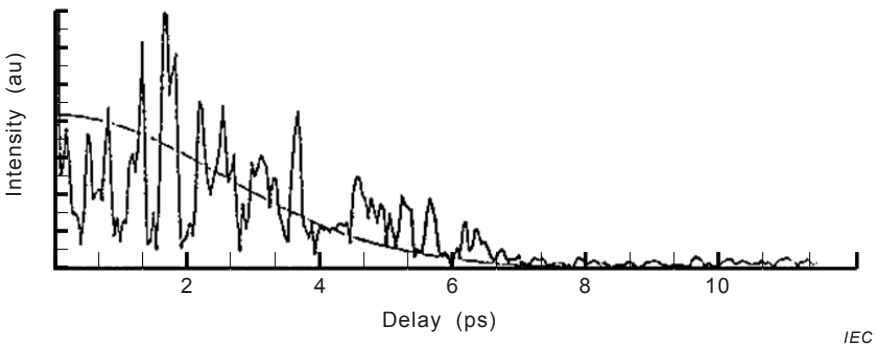

Figure 18 – Fourier transform

Figures 17 and 18 are a case of strong mode coupling and high PMD. For this case, IEC 61282-4-4 calls for calculating a weighted RMS using the $P(\tau)$ output function, avoiding the region near zero and the region in the noise, then takes the square root and reports it as the linear average – but without the $\sqrt{\frac{8}{3\pi}}$ multiplier.

For the case of negligible mode coupling, IEC 61282-4-4 treats the power values as a histogram of DGD values and a power weighted average is reported as the linear average. While this is not exactly correct, it may be adequate for simple birefringent elements.

5.5.4 Cosine Fourier transform

This mathematical development is based on the GINTY method that has been proven to produce the power-squared weighted PMD_{RMS}. It is found in IEC 60793-1-48 but not in any of the other International Standards. These calculations are most appropriate for high PMD, in which the extrema can be quite dense, as in Figure 17. For low to moderate PMD, when the ratio plot looks similar to Figure 16, the spectral differentiation technique (see 5.5.5) might be better.

Like the FT technique, the data must be available in equal frequency increments.

The windowing function, $W(v)$, is applied to the ratio of power difference (P_A-P_B) to power total (P_A+P_B). It should be clarified that when a broadband source is used, the windowing function can be set to the power total. In this case, the result will be equivalent to the GINTY.

The calculated interferograms for a given I/O-SOP, $E_{0i}(\tau)$ and $E_{xi}(\tau)$, are produced by fast cosine transforms on $W(v)$ and $W(v)R(v)$, respectively, where R is the ratio of power difference over power total. Following this, the calculations for GINTY are completed to produce spectral power-squared weighted PMD_{RMS}.

Doing the fast cosine Fourier transform includes frequency shifting that is not very well described in IEC 60793-1-48. The reason for frequency shifting is that the mathematics of GINTY include frequency integrals from 0.

The array put into the fast cosine transform algorithm must contain $n = 2^k+1$ elements. This will almost always be larger than the actual number of measurements. Frequency shifting results in placing the measurements into the input array and making the other elements equal to zero. The frequency shifting calculations will indicate where, in the array, the data should be placed.

Define $\Delta\nu$ as the frequency increment, e.g., in THz. The Nyquist frequency, ν_{NYQ}, is defined as Equation (108).

$$\nu_{NYQ} = n\Delta\nu \tag{108}$$

Find m, an integer, such that:

$$(m-1)\nu_{NYQ} \le \nu_{\min} < \nu_{\max} \le m\nu_{NYQ} \tag{109}$$

where $\nu_{\min}$ and $\nu_{\max}$ define the measured frequency boundaries.

The lower boundary for the Nyquist interval defined in Equation (109), the minimum measured frequency, and the frequency increment define the location within the input array for the first measured value.

After the fast cosine transform is done, the first element of the output array corresponds to time zero and the increasing elements correspond to increasing time, with increment, Δt, given as:

$$\Delta t = \frac{1}{2\nu_{NYQ}} \tag{110}$$

Because the cosine transform is even, the values at negative times are equal to the values of positive times.

When IEC 60793-1-48 is revised, it is recommended that the above material replace the region around Equations (A.13) and (A.14) of IEC 60793-1-48.

5.5.5 Spectral differentiation

This mathematical development is also based on the mathematics of GINTY. Instead of simulating interferograms, Equation (102) is used directly. This will be better suited to situations where there are a moderate number of extrema, but will generally need some fitting of the data.

In this subclause, optical frequency is expressed as angular optical frequency, ω, because the derivatives and integrals found in Equation (99) are with regard to this parameter.

Again, there is a windowing function $W(\omega)$ that is applied to the ratio of power differences to power total. For the broadband source, the windowing function can be the total power. For the tuneable laser case, a windowing function is still needed or the σ_0 parameter will disappear. The windowing function reflects the fact that the frequency extent is finite.

For a given I/O-SOP, $S_{0i}(\omega)$ and $S_{xi}(\omega)$ are given as $W(\omega)$ and $W(\omega)R(\omega)$. The data should generally be fitted to avoid noise and to yield the derivative functions, $\frac{dS_{0i}(\omega)}{d\omega}$ and $\frac{dS_{xi}(\omega)}{d\omega}$.

Calculate the power squared averages as:

$$\bar{S}_0^2(\omega) = \frac{1}{N}\sum S_{0i}^2(\omega) \quad \bar{S}_{0\omega}^2 = \frac{1}{N}\sum\left(\frac{dS_{0i}(\omega)}{d\omega}\right)^2 \quad \bar{S}_x^2(\omega) = \frac{1}{N}\sum S_{xi}^2(\omega) \quad \bar{S}_{x\omega}^2 = \frac{1}{N}\sum\left(\frac{dS_{xi}(\omega)}{d\omega}\right)^2 \tag{111}$$

These averages then need to be integrated with respect to frequency.

Calculate the RMS expressions as Equation (112):

$$\sigma_0^2 = \frac{\int \bar{S}_{0\omega}^2(\omega)d\omega}{\int \bar{S}_0^2(\omega)d\omega} \quad \sigma_x^2(\omega) = \frac{\int \bar{S}_{x\omega}^2(\omega)d\omega}{\int \bar{S}_x^2(\omega)d\omega} \tag{112}$$

The PMD_{rms} is now given as Equation (103).

5.6 Wavelength scanning OTDR and SOP analysis (WSOSA) method [7]

5.6.1 General

This method appears in IEC 61280-4-4. The method uses equations that are similar to those in the other test methods and in the theory; however, the notation of IEC 61280-4-4 and in [6] will be used for this subclause.

Figure 19 shows the setup.

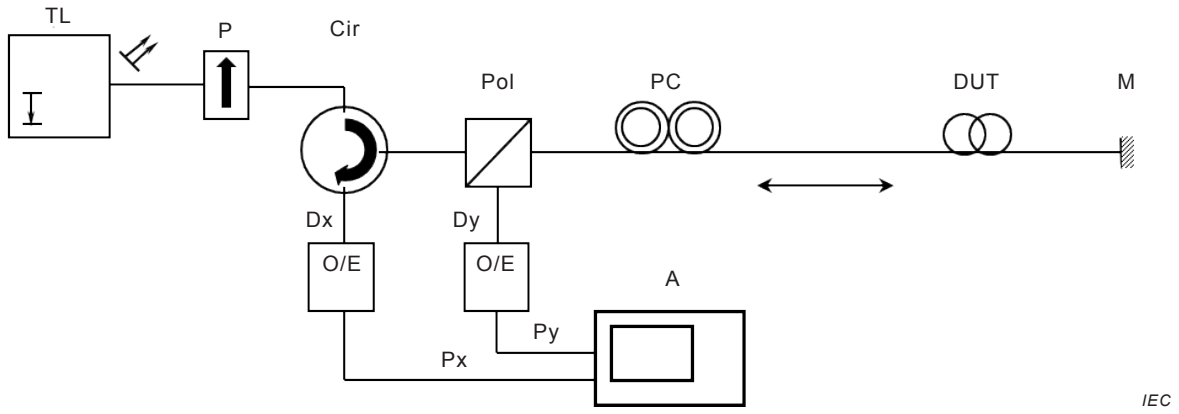

Key

TL pulsed tuneable light source
P polarizer
Cir circulator
Pol polarization beam splitter
PC I/O-SOP scrambler
M open connector or optical reflector
Dx, Dy detection system
A computer / analyzer

Figure 19 – WSOSA setup

The pulsed tuneable light source is synchronized with the detection system to capture the light reflected from the end of the DUT. This avoids the problem of capturing depolarized Rayleigh scattering light, an issue associated with 5.2.4. Some of the same math of 5.2.4 will be important for this method because the return path PMD (RMS) is calculated first, and the forward path PMD is then calculated using formulas similar to those in 5.2.4.

For a particular frequency, the pulses are typically averaged for some time to reduce noise. The effect of this averaging is interactive with the length of the pulse.

The optical frequencies for which reflected power, both P_x and P_y, is measured form an array of frequency pairs, as shown in Figure 20. The polarization scrambler settings are the same for both frequencies of a pair, but are randomized from one pair to the next. For each pair, a second, independent, pair of power measurements is measured using the same scrambler settings as the first pair of power measurements. This second pair of power measurements, marked with a prime, is used to minimize the effects of measurement noise.

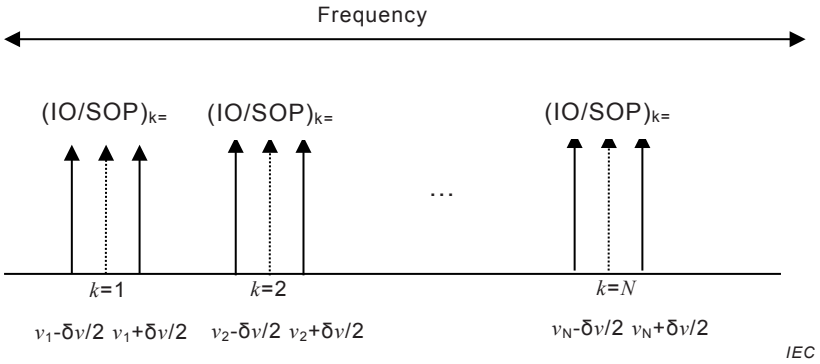

Figure 20 – Frequency grid

Just as all the frequency domain methods, the change in output SOP with frequency is the basis of the measurement. The overall range is typically around 12,8 THz with the number of frequency midpoints around 200.

In theory, any value of the source pulse width may be used, for instance from 10 ns to 20 μs. However, in practice, too short pulses will test only over shorter link lengths, unless the link is proportionally short; too long pulses may mix with several reflections; at the limit, this is exactly the case with continuous wave light sources.

The theory is based on the characteristics of the normalized transmission values, T, using formulas very similar to Equations (80) and (106). In Equation (113), the transmission value is dependent on the frequency pair, consequently the IO-SOP state, and the particular frequency of the pair.

$$T(\omega)=\frac{1}{2}\left(1+\vec{s}(\omega)\cdot\vec{s}_a\right)=\frac{1}{2}\left(1+s(\omega)\right)=\frac{1}{2}\left(1+\frac{P_x(\omega)-P_y(\omega)}{P_x(\omega)+P_y(\,)}\right)=\frac{P_x(\omega)}{P_x(\omega)+P_y(\omega)} \tag{113}$$

where

$\vec{s}(\omega)$ is the output Stokes vector at one of the frequencies of a pair;

$\vec{s}_a$ is random orientation of the analyser for the frequency pair;

s(ω) is the dot product;

$P_x(\omega)$ and $P_y(\omega)$ are the measured powers.

For each frequency of each pair, a second transmission value, T', is measured using the same time averaging and pulse length. This is used to reduce the noise effects in the mean squared difference calculation which is expressed as Equation (114).

$$\left\langle \Delta T^2 \right\rangle = \frac{1}{N} \sum_k \left(\Delta T_k * \Delta T_k' \right) \tag{114}$$

Where ΔT and $\Delta T'$ are the differences between transmission values for the two frequencies of the pair. The expected value operator in this case is over both IO/SOP and central frequency.

The noise reduction comes about by considering that the two terms on the right of Equation (114) can be considered as the true value plus a noise term. When the product is expanded, the parts of it with independent noise terms disappear in the sense of expected value.

The next subclauses will elaborate [7] in three parts:

- continuous model;
- large difference model;
- scrambling factor derivation.

The continuous model is needed to understand the large difference model. The scrambling factor derivation is needed for both.

There are constants in [7] that are somewhat different from those in IEC 61280-4-4. The main difference will be rationalized by considering that [6] works exclusively in terms of angular optical frequency, ω, while IEC 61280-4-4 is written in terms of frequency, v, where $\omega = 2\pi v$. 5.6.2 to 5.6.4 will be written in terms of angular optical frequency.

5.6.2 Continuous model

In the limit as $\delta\omega$ -> 0, and using Equations (113) and (18), the following equation can be derived:

$$\Delta T = \frac{1}{2}\left(\frac{ds}{d\omega} \right) \delta\omega = \frac{1}{2} \vec{s}_a \cdot \left(\vec{\Omega}_{RT} \times \vec{s} \right) \delta\omega \tag{115}$$

where

$\vec{\Omega}_{RT} = DGD_{RT}\vec{u}$ is the round trip PDV;

$\vec{u}$ is the round trip PSP.

Since the DGD is independent of the other terms, this allows writing Equation (116).

$$\left\langle \Delta T^2 \right\rangle = \frac{1}{4} \left\langle \left[\vec{s}_a \cdot \left(\vec{u} \times \vec{s} \right) \right]^2 \right\rangle_{IO-SOP} \left\langle DGD_{RT}^2 \right\rangle_w \delta\omega^2 \tag{116}$$

From 5.6.4, the term involving the Stokes vectors can be written as Equation (117).

$$\frac{1}{4} \left\langle \left[\vec{s}_a \cdot \left(\vec{u} \times \vec{s} \right) \right]^2 \right\rangle_{IO-SOP} = \frac{1}{15} \tag{117}$$

Consequently, the round trip PMD can be written as Equation (118).

$$PMD_{RT}^2 = \left\langle DGD_{RT}^2 \right\rangle_w = \frac{\alpha_{dT}^2 \left\langle \Delta T^2 \right\rangle}{\delta\omega^2} \tag{118}$$

where

$\alpha_{dT}^2 = 15$.

NOTE 1 In IEC 61280-1-4, there is a constant, α_{RS} = sqrt(15/4), that is the equivalent of α_{dT}. The factor of 4 is due to the fact that in IEC 61280-4-4, the division is by $\delta\nu$ rather than by $\delta\omega$.

From Equation (46), the forward PMD (RMS) is related to the return trip PMD as:

$$PMD_{F-RMS}^2 = \frac{3}{8} PMD_{RT}^2 \tag{119}$$

Using the relationship between RMS and linear average, Equations (24) and (25), the forward PMD linear average can be written as:

$$PMD_{F-AVG}^2 = \frac{1}{\pi} PMD_{RT}^2 \tag{120}$$

NOTE 2 Equations (119) and (120) depend on the assumption of random mode coupling and that the forward DGD follows a Maxwell distribution while the backward DGD follows a Rayleigh distribution. They are valid in the sense of expected value.

NOTE 3 Equations (119) and (120) are applicable to both the continuous model and the finite laser linewidth calculations of 5.6.3.

5.6.3 Large difference model

This clause leads to the actual formula for PMD_{RT} used in IEC 61280-4-4. It is based on an autocorrelation function that is defined as Equation (121) for a generalized random process, $y(\omega)$. It is defined so that $R_y(0) = 1$.

$$R_y(\omega_2 - \omega_1) = \frac{1}{\sigma_y^2}\left[\left\langle y(\omega_1) y(\omega_2)\right\rangle - \left\langle y\right\rangle^2\right] \tag{121}$$

The expression for the mean square difference with a finite frequency difference can be written as Equation (122).

$$4\left\langle \Delta T^2 \right\rangle = \left\langle \left(s(\omega_+) - s(\omega_-)\right)^2 \right\rangle = 2\left\langle s^2 \right\rangle - 2\left\langle s(\omega_+) s(\omega_-)\right\rangle \tag{122}$$

The ω_+ and ω_- symbols represent the upper and lower frequencies of a pair.

The common term for $\left\langle s(\omega_+)^2 \right\rangle$ and $\left\langle s(\omega_-)^2 \right\rangle$ is used because these expected values are independent of frequency.

A new variable, $x = s - \langle s \rangle$, which has zero mean, is introduced so Equation (122) can be rewritten as Equation (123).

$$2\left\langle \Delta T^2 \right\rangle = \left\langle s^2 \right\rangle - \left\langle s \right\rangle^2 - \sigma_x^2 \frac{\left\langle x(\omega_+)x(\omega_-) \right\rangle}{\sigma_x^2} = \sigma_s^2 \left[1 - R_x(\delta\omega)\right] \quad (123)$$

The term, σ_s^2, is the variance of s, which is the same as the variance of x. It has a value derived from polarization scrambling (see 5.6.4) and is used to define a constant, $\Delta T_0^2 = \sigma_s^2 / 2 = 8/45$, used in IEC 61280-4-4.

The autocorrelation function is the square of the Fourier transform of × in the limit as the frequency range goes to infinity. This is the same as the mean-square interferogram upon which the GINTY method is based. For randomly mode coupled fibres, this is Gaussian shaped, and hence, so is $R_x(\delta\omega)$.

The autocorrelation function is assumed to be Gaussian, of the form $\exp\left(-C^2\delta\omega^2\right)$, and is expanded in Taylor series to the second derivative.

$$R_z(\delta\omega) \approx 1 + R_x'(0)\delta\omega + \frac{1}{2}R_x''(0)\delta\omega^2 = 1 - C^2\delta\omega^2 \quad (124)$$

Combining Equation (124) and Equation (123), and considering that this combination shall yield the same result as Equation (116) for small δω, yields a value for C. This is shown in Equation (125).

$$\Delta T_0^2 C^2 \delta\omega^2 = \frac{PMD_{RT}^2 \delta\omega^2}{\alpha_{dT}^2} \quad (125)$$

The expression for the mean square difference using this expression of $R_x(\delta\omega)$ is Equation (126).

$$\left\langle \Delta T^2 \right\rangle = \Delta T_0^2 \left[1 - \exp\left(-\left(\frac{PMD_{RT}\delta\omega}{\alpha_{dT}\Delta T_0}\right)^2\right)\right] \quad (126)$$

Rearranging Equation (126) leads to Equation (G.12) of IEC 61280-4-4:2006 when the difference in frequency units is taken into account.

5.6.4 Scrambling factor derivation

This subclause will be used to establish the linkages used in 5.6.2 and 5.6.3. It is a restatement of Appendix A of [6].

In particular, the Stokes vectors $\vec{s}_{In}$, $\vec{s}_a$, and $\vec{s}$ represent the input Stokes vector, alignment of the analyser, and output Stokes vectors for ω, respectively (the dependence of the output Stokes vector on frequency is dropped for simplicity). These are related to the Jones vectors which are identified with the same subscripts.

The dot product, s, is given as Equation (127), using both bracket notation and the matrix notation used elsewhere. The second expression reads: two times j_a conjugate transpose times j (a complex scalar), multiplied by its conjugate, minus one.

$$s = \vec{s}_a \cdot \vec{s} = 2\left|\left\langle \vec{j}_a \middle| \vec{j} \right\rangle\right|^2 - 1 = 2\left(\vec{j}_a^{\uparrow} \vec{j}\right) * \left(\vec{j}_a^{\uparrow} \vec{j}\right)^* - 1 \tag{127}$$

Because the same random polarization is used in the forward and reverse directions, the following relationship is found for the input and analyser SOPs:

$$\vec{s}_a = \vec{s}_{In}^{\,0} = \begin{bmatrix} s_{In1} & s_{In2} & -s_{In3} \end{bmatrix}^T \Leftrightarrow \left|\vec{j}_a\right\rangle = \left|\vec{j}_{In}^{\,*}\right\rangle \tag{128}$$

NOTE 1 The * in the rightmost expression indicates conjugation only.

NOTE 2 The superscript 0 indicates the vector with the third element changed in sign.

Equations (127) and (128) lead to another expression for s that is given in terms of the Jones input to output matrix, T_{IO}. The subscript is here meant to distinguish the Jones matrix from the transmitted power.

$$s = 2\left|\left\langle \vec{j}_{In}^{\,*} \middle| T_{IO}^T T_{IO} \middle| \vec{j}_{In} \right\rangle\right| - 1 \tag{129}$$

The combined multiplication of T, T transpose, and input Jones vector yields the reflected output Jones vector.

The output Jones vector at the end of the fibre is designated as $\vec{j}_f$, with "f" indicating forward. It can also be written as the multiplication of T_{IO} and the input Jones vector as the left of Equation (130). The implication of conjugating is the right expression.

$$\left\langle \vec{j}_f \right| = \left\langle \vec{j}_{In} \middle| T_{IO}^{\uparrow} \Rightarrow \left\langle \vec{j}_{In}^{\,*} \middle| T_{IO}^T = \left\langle \vec{j}_f^{\,*} \right| \right. \right. \tag{130}$$

Substituting into Equation (129) results in Equation (131), the relationship of s with the output forward Stokes vector at the end of the fibre:

$$s = 2\left|\left\langle \vec{j}_f^{\,*} \middle| \vec{j}_f \right\rangle\right|^2 - 1 = \vec{s}_f^{\,0} \cdot \vec{s}_f \tag{131}$$

The value of s can therefore be given in terms of the third element of the output Stokes vector, with an implication for the frequency derivative as shown in Equation (132).

$$s = 1 - 2s_{f3}^2 \Rightarrow s' = -4s_{f3}s'_{f3} = -4s_{f3}\left(-\Omega_2 s_{f1} + \Omega_1 s_{f2}\right) \tag{132}$$

The $\varphi_{1,2}$ values are the first two elements of the forward PDV at the end of the fibre. The term that includes these values is derived from Equation (18).

From the derivative part of Equation (132), the IO-SOP expected value of the squared derivative is Equation (133).

$$\frac{\left\langle s'^2 \right\rangle_{IO-SOP}}{16} = \Omega_1^2 \left\langle s_{f2}^2 s_{f3}^2 \right\rangle_{IO-SOP} + \Omega_2^2 \left\langle s_{f1}^2 s_{f3}^2 \right\rangle_{IO-SOP} - 2\Omega_1\Omega_2 \left\langle s_{f1} s_{f2} s_{f3}^2 \right\rangle_{IO-SOP} \tag{133}$$

Since the input Stokes vector is uniformly distributed, so is the output forward Stokes vector, and the properties of the above expected values are solely determined by the properties of the scrambler. A uniform distribution of the input Stokes vector is equivalent to the following, where the parameter, a, is uniformly distributed between ±1 and the parameter, Φ, is uniformly distributed between $\pm\pi$.

$$\vec{s}_{In} = \begin{bmatrix} b\cos\phi & b\sin\phi & a \end{bmatrix}^T \quad b = \sqrt{1-a^2} \tag{134}$$

NOTE 3 The pdf of the elements of the input Stokes vector is $f(s) = [8(1\text{-}s)]^{1/2}$.

From these properties, the following expected value relationships can be demonstrated:

$$\left\langle s_i s_j \right\rangle = \begin{matrix} 0, i \neq j \\ 1/3, i = j \end{matrix} \tag{135}$$

$$\left\langle s_i s_j^2 \right\rangle = 0, i \neq j \tag{136}$$

$$\left\langle s_i^2 s_j^2 \right\rangle = \begin{matrix} 1/15, i \neq j \\ 1/5, i = j \end{matrix} \tag{137}$$

From the relationships in Equations (135) to (137) and Equation (133), Equation (138) emerges.

$$\left\langle s'^2 \right\rangle_{IO-SOP} = \frac{4}{15}\left[4\left(\Omega_1^2 + \Omega_2^2\right)\right] \tag{138}$$

From Equation (45), the expression of Equation (138) within the brackets is equal to the square of DGD_{RT}. Recalling that $T' = s'/2$, yields Equation (135), which is one way to write Equation (116). Here, the expected value is over both IO-SOP and frequency:

$$\left\langle T'^2 \right\rangle = \lim_{\delta\omega\to 0}\left\langle \frac{\Delta T^2}{\delta\omega^2} \right\rangle = \frac{1}{15} PMD_{RT}^2 \tag{139}$$

From the leftmost expression in Equation (132), the expected value and square of the expected value are given in Equation (140).

$$\left\langle s \right\rangle = \frac{1}{3} \quad \left\langle s^2 \right\rangle = \left\langle 1 - 4s_{f/3}^2 + 4s_{f/3}^4 \right\rangle = 1 - 4/3 + 4/5 = 7/15 \tag{140}$$

The variance of s and ΔT^2_0 are therefore given as Equation (141).

$$\sigma_s^2 = \left\langle s^2 \right\rangle - \left\langle s \right\rangle^2 = \frac{16}{45} \Rightarrow \Delta T_0^2 = \frac{8}{45} \tag{141}$$

This concludes the derivation of 5.6.2 and 5.6.3.

6 Limitations

6.1 General

It is the intent of Clause 6 to highlight some specific limitations to the test methods.

6.2 Amplified spontaneous emission and degree of polarization

Amplified spontaneous emission is caused by optical amplification and results in optical noise covering a significant spectrum. The noise leads to depolarization that can degrade the quality of PMD measurements. The standards call for a degree of polarization, which shall be measured at the output, of 90 % or more, but then state that degree of polarization as low as 25 % could be measured, but with a loss of accuracy.

Methods to mitigate depolarization due to optical amplifiers include:

- Control of OA saturation conditions

  This technique can be used most effectively with tuneable laser sources, which have higher power densities than some other sources. If the source can drive the amplifier into saturation, then noise is minimised and signal output maximised. This maintains both a good optical signal to noise ratio at the instrument detector and a large DOP for SOP measurements.

- Reducing the detection optical bandwidth

  The detector bandwidth can be limited to very effectively filter the noise. For example, the use of a tuneable optical filter at the detector, tracking in tandem with the source wavelength, allows a much lower noise power to arrive at the instrument. The detector is no longer subject to saturation, and the amount of noise affecting the wanted signal is reduced. The instrument performance is consequently maintained at higher optical signal-to-noise ratio levels.

- Reducing the detection electrical bandwidth

  The optical input must always be detected without the detector circuit becoming saturated or overloaded, or else PMD measurement linearity or bias problems occur. However, once the signal has been converted to an electrical signal, the electrical filtering methods can be used to limit the effective system bandwidth. This typically requires the light source to be modulated at a high frequency (e.g. when using the MPS method). This enables the signal power to be detected using tuned filters, synchronous demodulation, lock-in amplifier, etc., and the broadband noise is rejected except within the signal transmission window.

- Discriminating the light source from the noise

  This is essentially the same as reducing the electrical bandwidth, by modulating the source and detecting only the modulation, observed at the detector. The "modulation" may take many forms, typically intensity modulation, or digital keying or encoding methods.

6.3 Polarization dependent loss (or gain)

This is a phenomenon where the transmitted power at an optical frequency varies depending on the SOP launched into the fibre. It is $10\log10(T_{max}/T_{min})$, where T_{max}/T_{min} are the maximum and minimum transmitted powers.

IEC 61300-3-2 [8] contains measurement methods for use on components, one of which is "all states", which is a search over a large number of input states. Another method is based on launching Mueller states.

IEC 61280-4-4 states that none of the PMD test methods work when the PDL is in excess of 10 dB, but if the PDL is less than 1 dB, reasonable PMD results can be obtained. One of the aspects of PDL is that orthogonal input SOPs may no longer be orthogonal at the output.

The action of PDL can be understood somewhat, or evaluated, from consideration of Equation (35). First multiply the estimated T matrix by the missing complex constant, v_y, (either sign may be used). Then note that any matrix can be represented with a singular value decomposition, similar to Equation (3), as:

$$T = USV^* \tag{142}$$

The matrices U and V are orthonormal, and S is diagonal. When U = V, there is no PDL, the magnitude of the diagonal elements of S are one, and the result is the same as Equation (3). For the general case, where U is not equal to V, when the input Jones vector is equal to one of the columns of V, the output Jones vector is the corresponding column of U with power given as the square of the magnitude of the corresponding magnitude of S.

The output power is given as:

$$Pout = \vec{j}_{In}^{*} T^* T \vec{j}_{In} = \vec{j}_{In}^{*} V S^* S V^* \vec{j}_{In} \tag{143}$$

The eigenvalues of T^*T yield the T_{min} and T_{max} transmitted power which can then be converted to PDL.

6.4 Coherence effects and multiple path interference

Coherence interference effects and multiple path interference are also called Fabry-Perot effects or Fabry-Perot etalon effects.

Components, in particular, may contain bulk optical elements, fibre-waveguide splices, fibre-lens interfaces, etc. that can give rise to reflections due to optical index mismatch between elements.

The transfer function measurements are sensitive to cavity effects if the lengths of these cavities are shorter than the coherence length of the tuneable laser source. The longer the range between two reflections, the larger the effects will be. For instance, if two parasite reflections are separated by three metres of SMF, a fluctuation of a quarter of a wave of the cavity length will be enough to go from a maximum to a minimum in the transmission spectrum, approximately 0,25 μm in the SMF. A temperature fluctuation of the order of 0,01 °C may also be enough to generate such effects.

The effect of these reflections may also be to induce multi-path dispersions that are either PMD related (i.e. the path difference is polarization sensitive) or not (polarization insensitive path differences).

Reflections and multiple delay paths that are not polarization sensitive can be separately removed from $\Delta\tau$. Any kind of polarization-sensitive differential delay (birefringence effects), however, will affect the value reported as DGD.

6.5 Test lead fibres

The SMF test leads (sometimes called pigtails) add PMD of their own, which varies as the leads are bent, coiled or twisted.

The leads into and out of the transmission media (typically with little random coupling) always contribute some PMD.

NOTE Typical PMD values for a few meters of SMF are of the order of 1 fs/m or less. The PMD in the leads partially adds to, or partially subtracts from, the $\Delta\tau$ of the SMF component itself according to the axial alignment of the lead birefringence and that of the component.

Since the SMF leads are typically only a few meters long, the PMD in the leads is essentially deterministic, a source of uncertainty in the $\Delta\tau$ determination. This may be kept to a minimum by keeping the pigtails from being bent with a radius less than 50 mm to avoid bending birefringence being introduced. In addition, if required, the DGD measurements may be repeated many times, with the leads reconfigured each time to randomise the PMD contribution in the leads. The DGD will then be the average of the results taken. Care must be taken to ensure that the leads are arranged so that the full range of PMD variation is covered.

Devices with polarization maintaining fibre leads are normally highly polarization sensitive and the polarization axis of the device lead is aligned with the polarization axis of the device. Any misalignment will introduce significant PMD. In effect, these devices have high PDL.

It has been experimentally noticed that uncabled SMFs or loose-tube cabled SMFs may be preferred for test leads.

6.6 Aerial cables testing

Vibrations of the transmission media, such as may be induced by winds, lead to PMD measurement results that can be different from results that would be obtained without vibrations, depending on the rapidity of the measurement and the measurement method. The variation of the transmission matrices with optical frequency is confused with the variation from other sources.

It can be argued that if the transmission matrices are varying over the spectrum of the modulated signal due to something other than optical frequency and pure PMD, these effects will also lead to distortion.

Because of the optical transform, the effects are much reduced for the interferometric methods, but since it takes a finite time to complete a scan, they are still present. For the interferometric methods, the effects of vibration have been likened to polarization scrambling.

Depending on the measurement method, there are some different ways to quantify the stability of the transmission media – all of which involve multiple measurements.

Bibliography

[1] ITU-T G.sup39, G series, Supplement 39, "Optical system design and engineering considerations", 2012

[2] N. Gisin, B. Gisin, J.P. Von der Weid, and R. Passy, "How accurately can one measure a statistical quantity like Polarization Mode Dispersion", IEEE Photonics Technol. Lett., Vol. 8, N. 12, Dec.1996

[3] F. Corsi, A. Galtarossa, L. Palmieri, M. Schiano, T. Tambosso, "Continuous-Wave Backreflection Measurement of Polarization Mode Dispersion", IEEE Photonics Technol. Lett., Vol. 11, N. 4, April 1999, pp. 451-453

[4] P. Williams, "Modulation phase-shift measurement of PMD using only four launched polarization states: a new algorithm", Electronic Letters Online No: 19991068, DOI; 10.1049/EL:19991068,

[5] K. Sano, T. Kudou and T. Ozeki, "Simultaneous Measurement of Mode Group Delay Dispersion and Polarization Mode Dispersion", 22nd European Conference on Optical Communication – ECOC'96, Oslo

[6] N. Cyr, "Polarization-Mode Dispersion Measurement: Generalization of the Interferometric Method To Any Coupling Regime", JLT, 2003

[7] N. Cyr, H. Chen, and G. Schinn, "Random-Scrambling Tunable POTDR for Distributed Measurement of Cumulative PMD", JLT, 2009

[8] IEC 61300-3-2, Fibre optic interconnecting devices and passive components – Basic test and measurement procedures – Part 3-2: Examination and measurements – Polarization dependent loss in a single-mode fibre optic device

[9] IEC TR 61282-3, Fibre optic communication system design guides – Part 3: Calculation of link polarization mode dispersion

[10] IEC TR 61292-5, Optical amplifiers – Part 5: Polarization mode dispersion parameter – General information

———————

This page deliberately left blank

British Standards Institution (BSI)

BSI is the national body responsible for preparing British Standards and other standards-related publications, information and services.

BSI is incorporated by Royal Charter. British Standards and other standardization products are published by BSI Standards Limited.

About us

We bring together business, industry, government, consumers, innovators and others to shape their combined experience and expertise into standards -based solutions.

The knowledge embodied in our standards has been carefully assembled in a dependable format and refined through our open consultation process. Organizations of all sizes and across all sectors choose standards to help them achieve their goals.

Information on standards

We can provide you with the knowledge that your organization needs to succeed. Find out more about British Standards by visiting our website at bsigroup.com/standards or contacting our Customer Services team or Knowledge Centre.

Buying standards

You can buy and download PDF versions of BSI publications, including British and adopted European and international standards, through our website at bsigroup.com/shop, where hard copies can also be purchased.

If you need international and foreign standards from other Standards Development Organizations, hard copies can be ordered from our Customer Services team.

Subscriptions

Our range of subscription services are designed to make using standards easier for you. For further information on our subscription products go to bsigroup.com/subscriptions.

With **British Standards Online (BSOL)** you'll have instant access to over 55,000 British and adopted European and international standards from your desktop. It's available 24/7 and is refreshed daily so you'll always be up to date.

You can keep in touch with standards developments and receive substantial discounts on the purchase price of standards, both in single copy and subscription format, by becoming a **BSI Subscribing Member**.

PLUS is an updating service exclusive to BSI Subscribing Members. You will automatically receive the latest hard copy of your standards when they're revised or replaced.

To find out more about becoming a BSI Subscribing Member and the benefits of membership, please visit bsigroup.com/shop.

With a **Multi-User Network Licence (MUNL)** you are able to host standards publications on your intranet. Licences can cover as few or as many users as you wish. With updates supplied as soon as they're available, you can be sure your documentation is current. For further information, email bsmusales@bsigroup.com.

BSI Group Headquarters

389 Chiswick High Road London W4 4AL UK

Revisions

Our British Standards and other publications are updated by amendment or revision.

We continually improve the quality of our products and services to benefit your business. If you find an inaccuracy or ambiguity within a British Standard or other BSI publication please inform the Knowledge Centre.

Copyright

Useful Contacts:

Customer Services
Tel: +44 845 086 9001
Email (orders): orders@bsigroup.com
Email (enquiries): cservices@bsigroup.com

Subscriptions
Tel: +44 845 086 9001
Email: subscriptions@bsigroup.com

Knowledge Centre
Tel: +44 20 8996 7004
Email: knowledgecentre@bsigroup.com

Copyright & Licensing
Tel: +44 20 8996 7070
Email: copyright@bsigroup.com

bsi.